Published in final edited form as:
*Free Radic Biol Med*. 2007 March 15; 42(6): 738–737.

# Reduction of Hexavalent Chromium by Human Cytochrome $b_5$: Generation of Hydroxyl Radical and Superoxide

**Griselda R. Borthiry**[a], **William E. Antholine**[b], **B. Kalyanaraman**[b,c], **Judith M. Myers**[a], and **Charles R. Myers**[a,c,*]

***a*** *Department of Pharmacology and Toxicology, Medical College of Wisconsin, 8701 Watertown Plank Road, Milwaukee, WI 53226, USA*

***b*** *Department of Biophysics, Medical College of Wisconsin, 8701 Watertown Plank Road, Milwaukee, WI 53226, USA*

***c*** *Free Radical Research Center, Medical College of Wisconsin, 8701 Watertown Plank Road, Milwaukee, WI 53226, USA*

## Abstract

The reduction of hexavalent chromium, Cr(VI), can generate reactive Cr intermediates and various types of oxidative stress. The potential role of human microsomal enzymes in free radical generation was examined using reconstituted proteoliposomes (PLs) containing purified cytochrome $b_5$ and NADPH:P450 reductase. Under aerobic conditions, the PLs reduced Cr(VI) to Cr(V) which was confirmed by ESR using isotopically pure $^{53}$Cr(VI). When 5-Diethoxyphos-phoryl-5-methyl-1-pyrroline-*N*-oxide (DEPMPO) was included as a spin trap, a very prominent signal for the hydroxyl radical ($HO^{\bullet}$) adduct was observed as well as a smaller signal for the superoxide ($O_2^{\bullet -}$) adduct. These adducts were observed even at very low Cr(VI) concentrations (10 μM). NADPH, Cr(VI), $O_2$ and the PLs were all required for significant $HO^{\bullet}$ generation. Superoxide dismutase eliminated the $O_2^{\bullet -}$ adduct and resulted in a 30% increase in the $HO^{\bullet}$ adduct. Catalase largely diminished the $HO^{\bullet}$ adduct signal indicating its dependence on $H_2O_2$. Some sources of catalase were found to have Cr(VI)-reducing contaminants which could confound results, but a source of catalase free of these contaminants was used for these studies. Exogenous $H_2O_2$ was not needed, indicating that it was generated by the PLs. Adding exogenous $H_2O_2$, however, did increase the amount of DEPMPO/$HO^{\bullet}$ adduct. The inclusion of formate yielded the carbon dioxide radical adduct of DEPMPO, and experiments with dimethylsulfoxide (DMSO) plus the spin trap α-phenyl-*N*-*tert*-butylnitrone (PBN) yielded the methoxy and methyl radical adducts of PBN, confirming the generation of $HO^{\bullet}$. Quantification of the various species over time was consistent with a stoichiometric excess of $HO^{\bullet}$ relative to the net amount of Cr(VI) reduced. This also represents the first demonstration of a role for cytochrome $b_5$ in the generation of $HO^{\bullet}$. Overall, the simultaneous generation of Cr(V) and $H_2O_2$ by the PLs and the resulting generation of $HO^{\bullet}$ at low Cr(VI) concentrations could have important implications for Cr(VI) toxicity.

### Keywords

Hydroxyl radical; Chromium; Cytochrome $b_5$; Proteoliposomes; Free radical

Corresponding author: Dr. Charles R. Myers, Department of Pharmacology and Toxicology, Medical College of Wisconsin, 8701 Watertown Plank Road, Milwaukee, WI 53226, email: cmyers@mcw.edu, phone: 414-456-8593

## Introduction

Chromium (Cr) is an essential element that is present in a variety of environments in small amounts. Several industries use large amounts of chromium for a variety of applications including the production and use of chromate pigments, stainless steel machining and welding, zinc chromate primer paints, chrome plating, corrosion inhibition, leather tanning, and others. Exposure to hexavalent chromium, Cr(VI), is associated with numerous toxic effects, and contact with industrial Cr sources has provided valuable information on adverse effects in humans [1–8]. Environmental exposure to Cr is also of increasing concern. Greater than $10^5$ tons of Cr are released annually into the environment, and Cr is a significant contaminant at many sites across the U.S.A., including at hundreds of Superfund sites [9–11].

Cr(VI) and Cr(III) are the predominant stable oxidation states. Cr(III) compounds are generally insoluble and do not easily cross cell membranes [12], whereas many Cr(VI) compounds are highly soluble. Cr(VI) can readily cross the skin [13], and is transported into cells via an anion carrier [14]. Many in vitro studies have implicated exposure to Cr(VI) as the predisposing factor to Cr-induced genotoxicity [15–19]. The reduction of Cr(VI) to Cr(III), and the resulting formation of reactive intermediates (e.g. Cr(V), Cr(IV), reactive oxygen species), is likely a key component in the toxicity and carcinogenicity of Cr(VI) [18,20–24]. Reactive Cr intermediates, Cr(V) and Cr(IV), generated by some reductants can participate in Fenton-like reactions with hydrogen peroxide to generate hydroxyl radical [25–30].

Because the intracellular reduction of Cr(VI) is directly linked to its toxic effects, a complete understanding of the Cr(VI) reduction mechanisms is essential. Different intracellular Cr(VI) reductants could result in the generation of distinct types of reactive species, each mediating particular types of damage. Therefore, the mechanism(s) of Cr(VI) reduction, their location in the cell, and the rates of formation of the reactive intermediates will all influence the ultimate effects in cells. Studies using high concentrations of chemical reductants or various animal species have identified several possible Cr(VI) reductants, including ascorbate, cysteine, glutathione, glutathione reductase, rat microsomal enzymes, and others [28,31–35]. Many studies on the reductive activation of Cr(VI) have utilized animals, but key differences between humans and rodents have been reported with respect to the reductive activation of Cr(VI) [36,37]. A more thorough examination of Cr(VI) reduction in human systems, and its implications for toxicity, is therefore warranted.

The smooth endoplasmic reticulum (SER) is a major component of the isolated microsomal subcellular fraction. The SER is physically contiguous with the nuclear membrane and, in many cells, the SER represents the largest membrane surface area. The metabolism of hundreds of exogenous compounds has been attributed to microsomal enzymes. Among the most-studied enzymes with reductive capacity in the SER include cytochromes P450 and cytochrome $b_5$, and the flavoproteins P450 reductase and $b_5$ reductase. Previous studies demonstrated that microsomes from human liver and lung have prominent Cr(VI) reductase activity and generate both Cr(V) and Cr(IV) [36–39]. The effects of inhibitors are consistent with a prominent role for P450 reductase and $b_5$ reductase in the NADPH- and NADH-dependent Cr(VI) reductase activities, respectively [37,39], but these flavoproteins by themselves cannot account for the microsomal rates. Studies with NADH plus NADPH, relative to either alone, indicate that the flavoprotein reductases are donating electrons to a common component [39]. Inhibitor studies indicated that cytochromes P450 do not represent this common component [36,37]. However, both P450 reductase and $b_5$ reductase donate electrons to cytochrome $b_5$, and the addition of human cytochrome $b_5$ to microsomes significantly stimulates Cr(VI) reduction [36,39]. Proteoliposomes (PLs) containing either P450 reductase or cytochrome $b_5$ have limited to no capacity to reduce Cr(VI). However, PLs that contain both cytochrome $b_5$ and P450 reductase reduce Cr(VI), and generate Cr(V), under anaerobic conditions at rates which approximate

those 5 for microsomes [40]. While cytochrome $b_5$ was not examined, the intratracheal administration of Cr(VI) induces the expression of P450 reductase and $b_5$ reductase in rat lung by ≥ 2.4-fold [41].

Inhalation of Cr-containing fumes, dusts, and particles is a prominent form of exposure, so respiratory effects of Cr (pulmonary fibrosis, chronic bronchitis, and lung cancer) are of particular concern [5,7,42–45]. Aerobic conditions only inhibit a minority of Cr(VI) reduction by human microsomes [36,37] so the reductive activation of Cr(VI) could occur at significant rates in the lungs. The relative rates of Cr(VI) reduction by human liver vs. lung microsomes are consistent with their relative contents of cytochrome $b_5$ and P450 reductase [36,39]. In human lung, P450 reductase is primarily expressed in bronchial and bronchiolar epithelial cells [46]. While these epithelial cells are a minority of lung cells, their P450 reductase content could be higher than that of liver cells. These bronchial epithelial cells are directly exposed to inhaled toxins, including chromium, and are major sites of pulmonary tumors.

The goal of these studies was to determine if PLs containing human P450 reductase and cytochrome $b_5$ reduce Cr(VI) under aerobic conditions, and if this would result in the generation of reactive oxygen species (ROS). The reduction of Cr(VI) to Cr(V) was observed and confirmed with isotopically pure $^{53}Cr$. Spin trap studies demonstrated the generation of both $HO^{\bullet}$ and $O_2^{\bullet -}$ even at very low Cr(VI) concentrations (10 μM). NADPH, Cr(VI), $O_2$ and the PLs were all required for significant ROS generation. The identity of the $HO^{\bullet}$ was confirmed by multiple approaches. The generation of $HO^{\bullet}$ was dependent on $H_2O_2$, but exogenous $H_2O_2$ was not needed, indicating that the PLs generated sufficient $H_2O_2$. The various species were also quantified over time, including Cr(VI), Cr(V), and the $HO^{\bullet}$ and $O_2^{\bullet -}$ adducts of DEPMPO. These findings quantitatively support the redox cycling of at least a portion of the Cr to generate $HO^{\bullet}$.

In addition, it was discovered that some commercial sources of catalase have Cr(VI)-reducing contaminants which could confound interpretation of results in Cr-related studies.

## Materials and methods

### Chemicals and reagents

Purified recombinant human cytochrome $b_5$ and P450 reductase were purchased from Invitrogen Corp. (Carlsbad, CA). L-α-phosphatidylcholine, hydrogenated, egg yolk (cat. no. 840059) was purchased from Avanti Polar Lipids (Alabaster, AL). Sodium cholate was from Calbiochem (La Jolla, CA). Phenylmethylsulfonyl fluoride (PMSF) and Tris were from Research Organics (Cleveland, OH). Sodium chromate (99+%) was the highest purity available from Aldrich Chemical (Milwaukee, WI). Other chemicals obtained from Aldrich were activated aluminum oxide, activated carbon, 4-hydroxy-2,2,6,6-tetramethylpiperidine 1-oxyl, and 1,5-diphenylcarbazide. 5-Diethoxyphosphoryl-5-methyl-1-pyrroline-*N*-oxide (DEPMPO) was from Oxis International (Portland, OR), and α-phenyl-*N*-*tert*-butylnitrone (PBN) was from Alexis Biochemicals (Lausen, Switzerland). Ferrous ammonium sulfate and hydrogen peroxide were from Mallinckrodt Chemicals (Phillipsburg, NJ), and sulfuric acid was from J.T. Baker (Phillipsburg, NJ). Sodium chloride was from VWR Scientific (West Chester, PA) and EDTA was from Fisher Scientific (Hampton, NH). Three different catalases were obtained from Sigma (cat. no. C10, C30, C100) and two catalases were obtained from Calbiochem (cat. no. 219001 and 219008). The use of each catalase is specified in the results. All other chemicals and reagents were purchased from Sigma Chemical (St. Louis, MO).

## General procedures

To remove polyvalent metal ion contaminants, solutions were pretreated with Chelex-100 (5 g per 100 ml solution) for at least 1 hr before use.

Experiments under anaerobic conditions were conducted in an anaerobic chamber (Coy Laboratory Products, Grass Lake, MI) (4 to 5% $H_2$, balance $N_2$) as previously described [36]. Solutions were pre-incubated in the anaerobic chamber before use. Cr(VI) reduction rates under these conditions were found to be indistinguishable from those in which the vials were made anaerobic by flushing with $O_2$-free $N_2$ [36]. Experiments under aerobic conditions were conducted in open-top vials under room air.

## Preparation of Proteoliposomes

Proteoliposomes containing P450 reductase plus cytochrome $b_5$ were reconstituted using a procedure that was adapted from a published protocol [47]. Within the anaerobic chamber, an aliquot of egg yolk phosphatidylcholine (5 mg) in chloroform was placed in an iced 15-ml conical tube. The chloroform was removed by evaporation to dryness under a stream of $N_2$ at 37°C. Buffer (1.778 ml of 10 mM Tris-HCl, pH 7.2/50 mM NaCl/0.2 mM EDTA) was added to the dried lipids and they were vortexed vigorously for approximately 1 to 2 min to dislodge the dried lipid residue from the tube. Sodium cholate in water (10% w/v) was added to the lipid suspension to a final concentration of 1%. The solution was gently rocked for 1 hr at 4°C and then warmed in a 50°C waterbath for 5 to 10 min until the solution cleared. The liposomes were cooled and cytochrome $b_5$ was added followed by gentle rocking for 2 hr at 4°C. P450 reductase was then added followed by 1 hr rocking at 4°C. The molar ratio was 126/1.2/1.0 (lipid/cytochrome $b_5$/P450 reductase). These molar ratios were based on the mg of each component calculated from the concentrations provided by the manufacturers. The proteoliposomes were dialyzed in buffer (10 mM Tris-HCl, pH 7.2/50 mM NaCl/0.2 mM EDTA/1 mM PMSF) for a total of 6 hr (fresh buffer every 2 hr) using Slide-A-Lyzer mini dialysis units (10,000 MWCO, Pierce, Inc., Rockford, IL). They were stored at 4°C and used as soon as possible (usually within 1 day) for the experiments.

## Cytochrome $b_5$ Spectral Analysis

The reduction of cytochrome $b_5$ in proteoliposomes was followed spectrophotometrically at 37°C using either an Aminco DW2000 (SLM Instruments, Urbana, IL) or a Hitachi U-3310 (Tokyo, Japan) spectrophotometer. Proteoliposomes were diluted in 2.0 ml of 10 mM potassium phosphate buffer, pH 7.0, and the sample was vortexed for 10 sec under room air to ensure complete oxidation of cytochrome $b_5$. The sample was divided equally between sample and reference cuvets and was scanned once to establish the baseline. NADPH (final concentration of 0.2 mM) was added to the sample cuvet, which was mixed by inversion and then scanned four times (once every 2 min) from 400 to 700 nm. The resulting spectra represent the amount of cytochrome $b_5$ that can be reduced by NADPH:P450 reductase. An excess of sodium dithionite was then added to the sample cuvet, which was mixed by inversion and scanned again. This represents the total amount of cytochrome $b_5$. The difference in absorbance (peak minus trough) of the Soret peak was used to calculate the concentration of heme-containing cytochrome $b_5$ using the extinction coefficient 185 $mM^{-1}$ $cm^{-1}$ [48]. The amount of liposomes used for each experiment was normalized to this $b_5$ content.

## Electron Spin Resonance for Cr(V)

Cr(V) generation was examined at fixed time points using direct detection by ESR. Solutions were pre-treated with Chelex-100 resin for at least 1 hr prior to use. The buffer (final concentration in assay of 0.13 M KCl/2.17 mM potassium phosphate pH 7.35), water, and NADPH-generating mix [36] were pre-incubated for 5 min at 37°C. The PLs and $Na_2CrO_4$

were added followed by incubation at 37°C for the indicated times. The reaction was stopped by immersion in liquid nitrogen (77 K). Samples were stored in liquid nitrogen, typically for less than one week, until analysis by ESR. It was previously shown that Cr(V) is stable for at least several months at 77 K.

In order to match conditions used for spin trap experiments (below), samples were quickly thawed, placed in a quartz flat cell and ESR spectra were obtained without delay at room temperature using a Bruker EMX spectrometer. Instrument settings are indicated in the results. ESR spectra were confirmed in replicate experiments. The *g* values were determined by comparison to the 2,2,-diphenyl-1-picrylhydrazyl radical (DPPH) which has a *g* value of 2.0036.

## Electron Spin Resonance Spin Trapping

Reactive oxygen species were assessed at fixed time points using ESR spin trapping. The reagents and incubation conditions were identical to those described above for the Cr(V) ESR except that the spin trap DEPMPO (14 mM) was also included. The chromate and DEPMPO were added last. After the indicated 37°C incubation period, the samples were immersed and stored in liquid nitrogen. Freezing and thawing does not change the ESR spectra of DEPMPO adducts [49,50]. For ESR analysis, each sample was quickly thawed, placed in a quartz flat cell and ESR spectra were obtained without delay at room temperature using a Bruker EMX spectrometer. Instrument settings are indicated in the results. The spectra for each sample were stable during the ESR analysis time, with no noticeable changes in spectral intensity or pattern.

Experiments with proteoliposomes were initially done to compare two concentrations of DEPMPO (14 and 50 mM). The ESR spectral patterns and intensities were indistinguishable for these two DEPMPO concentrations, so 14 mM was used for subsequent studies to conserve spin trap. This is consistent with previous evidence on effective concentrations of DEPMPO [51]. ESR spectra were confirmed in replicate experiments. In some experiments, PBN was substituted for DEPMPO where indicated. All spectra were plotted on the same scales, except if indicated otherwise.

The hyperfine couplings were measured from the ESR scan data, and were confirmed using the simulation software WinSim (version 0.95) (National Institutes of Environmental Health Sciences) [52]. The concentration of each species was obtained by double integration of the simulated spectra using WinSim software. 4-hydroxy-2,2,6,6-tetramethylpiperidine 1-oxyl was used as the standard.

## Cr(VI) Reduction Assays

For some PLs preparations, ESR analyses for Cr(V) and DEPMPO adducts were done concurrently with experiments which followed the net loss of Cr(VI) over time. Two types of assays were used to quantify the amount of Cr(VI) reduced by the proteoliposomes. In the first, the decline in Cr(VI) was followed continuously over time at 37°C as a decrease in absorbance at 371 nm. Solutions were pre-treated with Chelex-100 resin for at least 1 hr prior to use. The buffer and reaction conditions were as described above for the ESR studies, except that the concentration of the $NADP^+$ was reduced to 0.2 mM in order to decrease possible spectral interference from NADPH. The buffer, water, NADPH generating mix and PLs were pre-incubated for 5 min to 37°C. The sample was divided equally between two cuvets (0.5 ml per cuvet). The assay was started by adding $Na_2CrO_4$ to the sample cuvet (an equal volume of water to the reference cuvet) and the absorbance at 371 nm was followed over time. The potential slow rate of Cr(VI) reduction by NADPH was determined by conducting the same experiment without PLs. The extinction coefficient of 3.2 $mM^{-1}$ $cm^{-1}$ was used to calculate the change in Cr(VI) concentration from the decline in absorbance at 371 nm. This extinction

coefficient was determined by adding different concentrations of a Cr(VI) (sodium chromate) standard to the NADPH generating mix/buffer that is used in these experiments, and immediately recording the absorbance at 371 nm. The absorbance centered at 340 nm for NADPH partially contributes to total absorbance at 371 nm, which necessitated determining the extinction coefficient under these conditions. The NADPH generating mix maintains a constant of level of NADPH over time and NADPH was in both cuvets so its relative contribution to the absorbance at 371 nm does not change over time during the experiments.

The concurrent ESR experiments similarly used this reduced concentration of $NADP^+$; there were no noticeable changes in the ESR signals when compared to those experiments which used 1 mM $NADP^+$ in the generating mix. While DEPMPO (14 mM) was included in the ESR spin trap experiments, it was not included in the final Cr(VI) reduction rate experiments in order to conserve spin trap. In preliminary studies, it was determined that there was not a noticeable difference in the Cr(VI) reduction rates in the presence vs. the absence of DEPMPO.

In some experiments, a colorimetric assay was used to verify Cr(VI) concentrations at fixed time points. The complete details of this 1,5-diphenylcarbazide colorimetric assay as applied to human enzymatic Cr(VI) reduction have been reported previously [37]. The only differences here were that the incubation buffer (0.15 M KCl/2.5 mM potassium phosphate, pH 7.35) was treated with Chelex-100 resin prior to use, and that proteoliposomes were substituted for microsomes. Volumes of all reagents were scaled down proportionally to accommodate smaller total reaction volumes.

For all assays, equivalent concentrations of PLs were used based on their cytochrome $b_5$ content as determined by the dithionite-reduced minus oxidized spectra described above.

## Results

### Reduction of Cytochrome $b_5$ in Proteoliposomes

A proteoliposome reconstitution procedure was previously described to facilitate electron transfer from NADPH to P450 reductase to cytochrome $b_5$ in vitro [40]. Here, a number of modifications were made to this procedure that significantly improved the consistency and efficiency of protein incorporation. Protein interaction in these PLs was determined by examining the extent of the NADPH-dependent reduction of cytochrome $b_5$ as determined by the intensity of the Soret peak in NADPH-reduced minus oxidized samples. Excess sodium dithionite was then added to reduce all of the cytochrome $b_5$, and the ratio between the NADPH- and dithionite-reduced spectra indicates the percentage of cytochrome $b_5$ that was reduced by NADPH:P450 reductase. In the example in Fig. 1, 79% of the cytochrome $b_5$ had been reduced in the presence of NADPH; for 14 different liposome preparations it was 83.4 ± 5.2% (mean ± S.D.). Previous studies showed that NADPH cannot donate electrons directly to cytochrome $b_5$ [40] so the electron transfer from NADPH to cytochrome $b_5$ is mediated by a successful functional interaction with P450 reductase.

### Generation of Cr(V)

Electron donors that transfer three electrons in a single step have not been identified in biological systems, so the reduction of Cr(VI) to Cr(III) must proceed stepwise through Cr(V) and/or Cr(IV). Cr(V), a $d^1$ paramagnetic species [53,54], can be directly detected by ESR spectroscopy by its sharp line spectrum ($g = 1.979$) at conventional X-band frequency. Previous studies demonstrated that human lung and liver microsomes generate Cr(V) during anaerobic Cr(VI) reduction [39]. Consistent with the transfer of one electron at a time by cytochrome $b_5$, PLs containing human cytochrome $b_5$ plus P450 reductase were similarly shown to generate Cr(V) under anaerobic conditions [40].

The central goal of this project was to examine the potential generation of reactive oxygen species as a result of aerobic Cr(VI) reduction by human $b_5$. The proteoliposomes generated Cr(V) ($g$ = 1.979) under aerobic conditions (Fig. 2A). The Cr(V) signal intensity was 70% smaller in the absence of proteoliposomes (Fig. 2B), which is consistent with previous results and is due to the slow rate of Cr(VI) reduction catalyzed by NADPH [39]. To confirm the authenticity of the Cr(V) signal, parallel studies were conducted with isotopically pure $^{53}Cr$ (stable isotope) as $Na_2{}^{53}CrO_4$. Because $^{53}Cr$ has a nuclear spin of I = 3/2, the single ESR line of Cr(V) was split into four lines (separation of 17.4 G) (Fig. 2C), typical for the hyperfine coupling for $^{53}Cr$(V) [53]. Analogous results were obtained with chromate concentrations of 100 μM and 10 μM (not shown) except that the signal intensities were smaller for 10 μM Cr (VI). Cr(V) species are potentially reactive and unstable and could be further reduced to Cr (IV) and/or Cr(III). Therefore, Cr(V) is a transient intermediate [39] and its signal intensity does not represent the total amount produced over time but rather the relative level at that point in time.

## Cr(VI) Reduction by Different Sources of Catalase

The generation of Cr(V) under aerobic conditions could potentially result in hydroxyl radical generation via Cr(V)-mediated Fenton-like chemistry [25–30]. Catalase was used as one of the tools (below) to determine if the reduction of $H_2O_2$ by reactive Cr intermediates was involved in hydroxyl radical formation. First, however, experiments were done to determine if catalase exhibited any Cr(VI) reductase activity which could complicate interpretation of the results. Two sources of catalase (Sigma C10 and Calbiochem 219008) catalyzed NADPH-dependent Cr(VI) reduction at significant rates. ESR studies were conducted with the Sigma C10 catalase and it was found that it generated Cr(V). Cr(VI) reduction is not an inherent property of catalase, however, as three other sources of catalase (Sigma C30 and C100, and Calbiochem 219001) did not exhibit detectable NADPH-dependent Cr(VI) reduction. The two catalases that had Cr (VI) reductase activity must therefore have contained one or more contaminants (identity unknown) that catalyzed the NADPH-dependent activity. None of the five catalases had significant rates of Cr(VI) reduction in the absence of NADPH. To avoid potential complications in our studies, Sigma C100 catalase was used for the remaining experiments because it does not reduce Cr(VI) under the experimental conditions.

## Spin Trapping of Hydroxyl Radical

5-Diethoxyphosphoryl-5-methyl-1-pyrroline-*N*-oxide (DEPMPO) was used to trap and detect hydroxyl radical by ESR. Unlike 5,5,-dimethylpyrroline *N*-oxide (DMPO), DEPMPO can trap and stabilize hydroxyl radical as DEPMPO/$^{\bullet}$OH and superoxide as DEPMPO/OOH, giving ESR spectra characteristic of each [49]. The DEPMPO/OOH adduct is 15 times more persistent than the DMPO/OOH adduct [49], and DEPMPO/OOH does not spontaneously decay to DEPMPO/$^{\bullet}$OH [49,55].

Experiments were conducted under aerobic conditions to determine the potential generation of hydroxyl radical as a result of NADPH-dependent Cr(VI) reduction by proteoliposomes. Following a 10 min incubation under aerobic conditions with 100 μM chromate, the NADPH-generating mix, and DEPMPO, the signal in Fig. 3A was observed. The most prominent component of this signal is the hydroxyl radical adduct of DEPMPO (DEPMPO/$^{\bullet}$OH) (8-line spectrum with an intensity ratio of 1:2:2:1:1:2:2:1) which matches that observed for the positive control for hydroxyl radical (ferrous iron plus $H_2O_2$, Fig. 3B). The other components of this signal align with those of a superoxide positive control (xanthine plus xanthine oxidase, Fig. 3C). The Fig. 3C spectrum is largely that of the superoxide adduct, but it does contain a lesser signal corresponding to the hydroxyl radical adduct. The Fig. 3A spectrum suggests that, under these conditions, the proteoliposome system generates both superoxide and hydroxyl radical.

Additional experiments were conducted to further define the identity of the superoxide adduct component (DEPMPO/OOH). When superoxide dismutase (SOD) was added to this proteoliposome system, the signal for DEPMPO/OOH largely disappeared whereas that for DEPMPO/$^{\bullet}$OH remained, and in fact increased by 30% (Fig. 3D). This increase in DEPMPO/$^{\bullet}$OH is consistent with the ability of superoxide to directly react with spin adducts, converting them to ESR silent species [56,57]. SOD accelerates the conversion of superoxide to $H_2O_2$. The hyperfine coupling constants for the spectrum in Fig. 3D ($a^P$ = 47.2 G, $a^H$ = 13.8 G, $a^N$ = 13.8 G) are consistent with those reported for DEPMPO/$^{\bullet}$OH [58] and were essentially the same as those measured for the authentic hydroxyl radical (Fig. 3B). The inclusion of both SOD and catalase resulted in a large decline in the signal intensities for DEPMPO/OOH and DEPMPO/$^{\bullet}$OH, with the Cr(V) signal predominant (Fig. 3E). When Cr(VI) was excluded, the Cr(V) signal was absent, but a small spin adduct signal was observed which contained components for both DEPMPO/$^{\bullet}$OH and DEPMPO/OOH (Fig. 3F). The DEPMPO/OOH component of the Fig. 3F spectrum largely disappeared when SOD was included, leaving only a tiny DEPMPO/$^{\bullet}$OH signal (Fig. 3G). Additional minor components in the Fig. 3G spectrum suggested traces of one or more unidentified species.

Additional experiments were conducted to further explore the hydroxyl radical component of the signal. The spectrum generated by the PLs following a 10 min incubation with 50 μM chromate is shown in Fig. 4A. Catalase, which should largely inhibit the formation of hydroxyl radical from $H_2O_2$, reduced the DEPMPO/$^{\bullet}$OH signal intensity significantly (Fig. 4B), while the superoxide adduct signal remained. Formate is oxidized by hydroxyl radical to yield a carbon dioxide radical anion which can be trapped as DEPMPO/$CO_2^{\bullet -}$ [58]. In the presence of 250 mM formate, the DEPMPO/$^{\bullet}$OH signal was largely replaced with that of DEPMPO/$CO_2^{\bullet -}$ (Fig. 4C), whereas the superoxide component of the signal remained. The overall increased signal intensity in the presence of formate (Fig. 4C) is attributed to an increased stability of the DEPMPO/$CO_2^{\bullet -}$ adduct relative to that of the DEPMPO/$^{\bullet}$OH adduct (Fig. 4A). The ESR spectra were essentially flat when the NADPH-generating mix was excluded (Fig. 4D) and only tiny amounts of adducts were observed when the PLs were omitted (Fig. 4E). The weak signals observed in the absence of liposomes could result from the slow rate of Cr (VI) reduction catalyzed by NADPH (see Fig. 2) [39]. Analogous results were obtained with different Cr(VI) concentrations, specifically 100 μM (Fig. 3 and not shown) and 10 μM (Fig. 4F through J) except that the signal intensities were smaller for 10 μM Cr(VI). Also, with 10 μM Cr(VI), the DEPMPO/OOH component of the spectrum was more prominent than that for DEPMPO/$^{\bullet}$OH (Fig. 4F). In total, the results in Figures 3 and 4 indicate that the NADPH-dependent reduction of Cr(VI) by the PLs results in the generation of hydroxyl radical. NADPH, PLs, and Cr(VI) are all required for significant hydroxyl radical formation. The catalase results are consistent with $H_2O_2$ supporting hydroxyl radical generation from a Fenton-like reaction of reactive Cr intermediates, e.g. Cr(V) and/or Cr(IV). It should be noted that exogenous $H_2O_2$ was not added to these experiments, indicating that the proteoliposome system generates sufficient $H_2O_2$ to support hydroxyl radical formation. Given that superoxide was also detected, it is possible that superoxide dismutation served as the source for at least some of the $H_2O_2$.

The Cr(V) signal (Fig. 2A, 3E) is located at the high-field end of the 8-line spectrum for DEPMPO/$^{\bullet}$OH (e.g. Fig. 3A, 4A, and 4B) making it difficult to visualize Cr(V) and the DEPMPO adducts simultaneously. Analogous experiments were therefore conducted in which $^{53}CrO_4^{2-}$ was substituted for $CrO_4^{2-}$ (Fig 5). While the two low-field lines for $^{53}$Cr(V) are not easily seen because they are within the DEPMPO/$^{\bullet}$OH spectrum, the two high-field lines for $^{53}$Cr(V) can be seen to the right of the DEPMPO/$^{\bullet}$OH spectrum (Fig. 5C,D), confirming the presence of Cr(V) under aerobic conditions in the presence of DEPMPO. When $^{53}CrO_4^{2-}$ (Fig. 5C,D) was substituted for $CrO_4^{2-}$ (Fig 5A,B), it was also noted that the

intensity of the high-field line for DEPMPO/$^{\bullet}$OH was more similar to that of its low-field line because the $^{53}$Cr(V) signal is not coincident with the high-field line for DEPMPO/$^{\bullet}$OH.

It has been noted that 4 mM deferoxamine (DFX) reduces the amount of Cr(V) detected during Cr(VI) reduction by NADPH and by glutathione reductase, and that DFX also inhibits Cr(V)-mediated Fenton-like reactions with $H_2O_2$ [30]. The effects of DFX on the proteoliposome system were therefore explored. The three concentrations of DFX examined (0.1, 0.25, and 0.75 mM) all caused a marked decline (68–81%) in the levels of DEPMPO/$^{\bullet}$OH adducts (Fig. 6). These declines in DEPMPO/$^{\bullet}$OH were significant ($P < 0.001$). In experiments without DEPMPO, DFX similarly eliminated the vast majority of the Cr(V) ESR signal (not shown). These results imply that Cr(V) is required, either directly or indirectly, for the generation of hydroxyl radical by the proteoliposomes. It was also noted that DFX caused an increase in the superoxide adduct signal intensities but these increases were not significant ($P > 0.05$) (Fig. 6).

## Dimethylsulfoxide to Confirm Hydroxyl Radical Formation

To confirm the generation of hydroxyl radical in this system, additional experiments were performed using a secondary radical trapping technique in which α-phenyl-*N*-*tert*-butylnitrone (PBN) was used as a spin trap and dimethylsulfoxide (DMSO) as a hydroxyl radical scavenger. Hydroxyl radical reacts with DMSO to yield a methyl radical ($^{\bullet}CH_3$):

$$(CH_3)_2SO + {}^{\bullet}OH \rightarrow {}^{\bullet}CH_3 + CH_3SO_2H \quad (1)$$

and PBN forms long-lasting spin adducts of carbon-centered radicals. PBN does not react with Cr(V) at pH 7.4 [59]. As shown above, the NADPH-dependent reduction of chromate by PLs yielded a composite spectrum of DEPMPO/$^{\bullet}$OH and DEPMPO/OOH (Fig. 7A,F). When PBN was substituted for DEPMPO, the Cr(V) signal was observed in addition to a small 6-line signal whose hyperfine coupling constants ($a^N = 15.40$ G, $a^H = 2.74$ G) are consistent with PBN/$^{\bullet}$OH (Fig. 7B,G) [60]. The small size of the PBN/$^{\bullet}$OH signal reflects the unstable nature and short-half life of oxygen-based adducts of PBN [60–62]. Both the PBN/$^{\bullet}$OH and Cr(V) signals were dependent on NADPH (Fig. 7C,H). In the absence of PLs, there was no PBN/$^{\bullet}$OH signal and only a small Cr(V) signal (not shown). When both DMSO and PBN were included with PLs, a spectrum was observed whose most prominent component had hyperfine coupling constants ($a^N = 15.05$ G, $a^H = 3.32$ G) that are consistent with those for the methoxy radical ($^{\bullet}OCH_3$) adduct of PBN (Fig. 7D,I), and are inconsistent with those for PBN/$^{\bullet}$OH [62,63]. However, closer inspection of this spectrum (Fig. 7L) revealed a second component whose hyperfine constants ($a^N = 16.51$ G, $a^H = 3.68$ G) matched those of the simulated PBN/$^{\bullet}CH_3$ adduct (Fig. 7K). The major component in the Fig. 7L spectrum aligned closely to that of the simulation for the PBN/$^{\bullet}OCH_3$ adduct (Fig. 7M). The addition of catalase resulted in a large diminution of the PBN/$^{\bullet}OCH_3$ signal, whereas the Cr(V) signal increased (Fig. 7E). A PBN-methoxy radical spectrum analogous to that in Fig. 7D was obtained when the Fenton reaction (ferrous iron plus $H_2O_2$) was conducted with PBN plus DMSO under room air, whereas a PBN-methyl radical signal was obtained under anaerobic conditions (not shown).

Simulation of the spectra for five experiments with PBN plus DMSO, using varied concentrations of Cr(VI) (10, 50, or 100 μM) yielded the relative amounts of the PBN adducts: 73 ± 3.0 % PBN/$^{\bullet}OCH_3$ and 27 ± 3.0% PBN/$^{\bullet}CH_3$. In these experiments with DMSO, PBN/HO$^{\bullet}$ comprised only 0.3 ± 0.06% of the total PBN adducts. A preponderance of PBN/$^{\bullet}OCH_3$ in preference to PBN/$^{\bullet}CH_3$ has been observed for three other methods of hydroxyl radical generation in air-saturated aqueous solutions under room air in the presence of DMSO [62]. The rate constants predict that methoxy radical adducts are favored over methyl radical adducts

under these conditions, i.e. methyl radical reacts much more readily with $O_2$ than with PBN [64]. Our findings are consistent with these predictions and previous observations.

When [$^{13}C_2$]DMSO was substituted for [$^{12}$C]DMSO, splittings from the $^{13}$C (I = 1/2) were observed in the PBN/$^{\bullet}CH_3$ component of the spectrum (not shown), confirming the methyl radical identity and therefore the generation of hydroxyl radical. Splittings were not observed in the PBN/$^{\bullet}OCH_3$ component of the spectrum; this is expected given that the $^{\bullet}OCH_3$ radical is oxygen-centered. Together, these results with PBN and DMSO confirm the generation of hydroxyl radical during the NADPH-dependent reduction of Cr(VI) by the PLs.

## ESR Spectra: Aerobic vs. Anaerobic Conditions

Sugden and Wetterhahn [59] reported that the spin trap 5,5,-dimethylpyrroline *N*-oxide (DMPO) can react directly with reactive Cr species, e.g. Cr(V), to generate ESR spectra resembling DMPO/$^{\bullet}$OH, and that the reaction does not involve the formation of diffusible hydroxyl radical. Experiments were therefore conducted to determine if DEPMPO might similarly react with proteoliposome-generated Cr(V), which could complicate interpretation of the DEPMPO/$^{\bullet}$OH signals. There were distinct differences in the ESR spectra when experiments were conducted under anaerobic versus aerobic conditions (Fig. 8). In contrast to aerobic conditions in which the DEPMPO/$^{\bullet}$OH signal predominates (Fig. 8E), Cr(V) is the predominant signal under anaerobic conditions with only a small signal from DEPMPO adducts (Fig. 8A). The anaerobic signal is also more complex than that of DEPMPO/$^{\bullet}$OH or DEPMPO/OOH suggesting small quantities of additional unknown species. The aerobic spectra with catalase (Fig 8F) and formate (Fig 8G) are consistent with hydroxyl radical formation requiring $H_2O_2$, whereas the anaerobic data show little, if any, effect of catalase on the small DEPMPO components of the spectrum (Fig. 8B). The anaerobic data with formate (Fig. 8C) suggest a small amount of DEPMPO/$^{\bullet}CO_2^-$, which could indicate trace amounts of hydroxyl radical production under anaerobic conditions. The most likely source would be small amounts of residual oxygen in either the liposomes or the NADPH-generating solutions that are prepared fresh and brought into the anaerobic chamber shortly before use. When the NADPH-generating mix was excluded from the reactions, the ESR spectra were essentially flat (Fig. 8D,H). Altogether, the large differences between the aerobic and anaerobic spectra demonstrate that essentially all of the DEPMPO/$^{\bullet}$OH signal observed under aerobic conditions results from hydroxyl radical and that $O_2$ is required. The DEPMPO/$^{\bullet}$OH signal observed under aerobic conditions is not due to a reaction between Cr(V) and DEPMPO because, if it were, it would also have been observed under anaerobic conditions in which Cr(V) was generated.

## Quantification of Various Species Over Time

ESR spectra were collected at various time points (between 1 min and 60 min) to assess the relative changes in Cr(V) and the DEPMPO adducts of $O_2^{\bullet -}$ and HO$^{\bullet}$ (Fig. 9). The concentrations of each were estimated from simulation of the spectra from replicate experiments, and were compared with the net reduction of Cr(VI) (Fig. 9). Experiments were conducted either without $H_2O_2$ (Fig. 9A) or with the inclusion of 2 mM $H_2O_2$ (Fig. 9B). Note that Cr(VI) is plotted on a different scale from the other species. At all time points, DEPMPO/$^{\bullet}$OH was the most abundant ESR species, with DEPMPO/OOH the second most abundant (Fig. 9A, B).

In the absence of $H_2O_2$, the mean levels of both DEPMPO/$^{\bullet}$OH and DEPMPO/OOH remained fairly constant over time, ranging from 5.5 to 11.6 μM DEPMPO/$^{\bullet}$OH and 2.4 to 4.2 μM DEPMPO/OOH (Fig. 9A). The variability among replicates for these two species was greatest during the first 5 min, with comparatively little variability thereafter (Fig. 9A). The net rate of Cr(VI) reduction declined progressively over time (Fig. 9A), with the highest rate (3.3 μM per min) during the first minute, and the slowest rate (0.15 μM per min) during the last 10 min.

In the presence of 2 mM $H_2O_2$, the levels of DEPMPO/•OH (12.9 to 23.4 μM) (Fig. 9B) were approximately twice as high as those seen without $H_2O_2$ (Fig. 9A). The levels of DEPMPO/•OH were significantly greater in Fig. 9B than those in Fig. 9A for all time points from 15 min to 40 min ($P < 0.01$) and also for the 50 min samples ($P < 0.05$). The mean levels of DEPMPO/•OH increased during the first five minutes and remained relatively constant thereafter (Fig. 9B). The level of DEPMPO/OOH remained fairly constant over the entire time course (5.5 to 7.7 μM). Similar to Fig. 9A, the net rate of Cr(VI) reduction decreased progressively over time (Fig. 9A).

While difficult to see on the graphs, the simulations indicated small amounts (0.1 to 0.28 μM) of Cr(V) at all time points in Fig. 9A and 9B. The lack of accumulation of Cr(V) over time under aerobic conditions indicates that it is a transient intermediate with a limited half-life. However, Cr(V) is also a transient intermediate under anaerobic conditions, but significantly higher levels of Cr(V) were observed anaerobically (Fig. 7) [40]. The Cr(V) levels are likely lower under aerobic conditions because some of the Cr(V) is also re-oxidized to Cr(VI) leading to hydroxyl radical generation [25,26,28]:

$$\mathrm{Cr(V)} + \mathrm{H_2O_2} \rightarrow \mathrm{Cr(VI)} + \mathrm{HO^{\bullet}} + \mathrm{OH^{-}} \quad (2)$$

The re-oxidation of Cr(V) to Cr(VI) during this reaction would have the overall effect of slowing the net rate of Cr(VI) reduction, and could potentially lower Cr(V) levels under conditions which support hydroxyl radical generation. In support of this, the Cr(V) levels were significantly less in the presence of $H_2O_2$ (Fig. 9B) than in its absence (Fig. 9A) during the first 30 min of incubation. Similarly, the mean rate of Cr(VI) reduction was modestly slower over the first 30 min in Fig. 9B when compared to Fig. 9A. However, these Cr(VI) differences were not statistically significant. This is likely because the differences in Cr(V) were less than 0.2 μM, which is within the variability of the Cr(VI) assay. Also consistent with reaction *2* is the observation that the Cr(V) signal intensity was increased in the presence of catalase (Fig. 7E).

The redox cycling of at least some of the Cr under aerobic conditions could theoretically result in a stoichiometric excess of HO• generation relative to the net amount of Cr(VI) reduced, provided that sufficient $H_2O_2$ was available. This was examined by comparing the molar ratio of the DEPMPO/•OH adduct at each time point to the total net amount of Cr(VI) loss from time zero to each time point (Fig. 9C). Ratios greater than 1.0 indicate a stoichiometric excess of HO• generation relative to net Cr(VI) loss. In the absence of added $H_2O_2$, this ratio was 2.8 at the earliest time point and remained above 1.0 for the first 5 min. When $H_2O_2$ was added, these ratios were significantly higher, starting at 6.3 for the earliest time point and remaining above 1.0 for the first 30 min. These ratios are consistent with a stoichiometric excess of HO• generation during the earlier time points. Since the Cr(VI) loss is similar under both conditions, the higher ratios with $H_2O_2$ represent larger amounts of DEPMPO/•OH adducts under these conditions. The PLs can therefore generate sufficient $H_2O_2$ to support a stoichiometric excess of HO• at the early time points, but additional $H_2O_2$ supports additional redox cycling of the Cr.

## Discussion

The cholate dialysis proteoliposome procedure used in these studies yielded liposomes with dependable protein incorporation and consistent reaction rates, with the vast majority of cytochrome $b_5$ typically reduced by NADPH:P450 reductase. Efficient electron transfer from P450 reductase to $b_5$ only occurs when both proteins are optimally tethered to the same face of the membrane by their hydrophobic amino- and carboxy-terminal domains, respectively. The data indicate that most of each protein must be tethered to the outer face of the liposomes

because NADPH does not readily diffuse across membranes. Similarly, chromate only crosses membranes by an anion carrier [14], so the ability to reduce Cr(VI) implies that the majority of cytochrome $b_5$ must be tethered to the outer face of the PLs.

Since the lungs are a primary target for occupational Cr(VI) exposure, Cr(VI) reduction under aerobic conditions is of interest. The studies reported here demonstrate that PLs containing human cytochrome $b_5$ plus P450 reductase reduce Cr(VI) under aerobic conditions. This is consistent with the previous reports on Cr(V) formation by human lung and liver microsomes and by PLs under anaerobic conditions [39,40]. The formation of Cr(V) is consistent with the ability of cytochrome $b_5$ to transfer one electron at a time. Cr(V) is a transient intermediate [39] with several possible fates: (a) it can directly react with cellular components [65]; (b) it can be oxidized by hydrogen peroxide generating hydroxyl radical and regenerating Cr(VI); or (c) it can be further reduced to Cr(IV) and/or Cr(III). Human microsomes reduce some of the Cr(V) to Cr(IV) under anaerobic conditions [39], but it remains to be determined if the proteoliposomes also generate Cr(IV).

Several lines of evidence support the generation of significant amounts of hydroxyl radical during Cr(VI) reduction under aerobic conditions.. The DEPMPO/$^{\bullet}$OH adduct signal was predominant and its hyperfine constants matched those for authentic DEPMPO/$^{\bullet}$OH. The DEPMPO/$^{\bullet}$OH spectrum is not the result of a possible reaction of Cr(V) with DEPMPO. In the presence of formate, the DEPMPO/$^{\bullet}$OH adduct was largely replaced with that of DEPMPO/$^{\bullet}CO_2^-$. When PBN was used as a spin trap, the PBN/$^{\bullet}$OH adduct was detected, and with PBN plus DMSO both PBN/$^{\bullet}CH_3$ and PBN/$^{\bullet}OCH_3$ adducts were generated. The use of [$^{13}C_2$]DMSO confirmed the identity of the methyl radical adduct. Catalase largely diminished the DEPMPO/$^{\bullet}$OH signal, whereas superoxide dismutase did not. Superoxide dismutase did, however, significantly decrease the DEPMPO/OOH signal intensity. Both the DEPMPO/OOH and DEPMPO/$^{\bullet}$OH signals were dependent on the presence of $O_2$. Together, the evidence is consistent with the NADPH-dependent reduction of Cr(VI) to reactive Cr species which can generate hydroxyl radical from Cr-mediated Fenton-like reactions.

While there are a number of reports on the generation of hydroxyl radical by partially reduced Cr species, there are several noteworthy aspects of the proteoliposome system used here. One is that the nature of the Cr(V) generated by $b_5$ (tetrahedral oxyanion) is different from the GSH-Cr(V), cysteine-Cr(V), or artificial 'stable' Cr(V) complexes that have been used in some other studies. These differences could influence the reactivity of these Cr species and might have implications for the resulting types of damage. The second point is the direct involvement of microsomal enzymes. To our knowledge, this is the first report on a role for cytochrome $b_5$ in hydroxyl radical generation. Another noteworthy aspect is the low concentration of Cr(VI) and reductants. Hydroxyl radical was generated at all Cr(VI) concentrations tested (100, 50, and 10 μM). These are well below those used in most studies in which chromate/dichromate concentrations have typically been 1 to 2 mM [25–30,34,66]. One study with glutathione reductase did note hydroxyl radical generation when using insoluble $PbCrO_4$ at 50 μg per ml (equivalent to 155 μM) [67]. While the minimal required Cr(VI) concentration to support hydroxyl radical generation has typically not been reported, it is clear from the cytochrome $b_5$ studies reported here that hydroxyl radical generation occurs even with low μM Cr. This is in agreement with observations with A549 cells, in which 10 μM Cr(VI) caused a 1.4-fold increase in the DMPO/OH adduct signal intensity [68]. This increase was abolished by SOD and catalase [68], suggesting that it was related to ROS production, although the relative contributions of superoxide and hydroxyl radical to the signal were not clear.

In studies using chemical reductants of Cr(VI) (e.g. ascorbate, glutathione, α-lipoic acid, NADPH, cysteine) to assess hydroxyl radical generation, concentrations of reductants have typically been 2 to 50 mM [25,27,29,34,66]. In studies with other Cr(VI)-reducing enzymes,

enzyme concentrations have often been given as units of activity based on specific enzyme substrates. Direct comparisons to cytochrome $b_5$ are difficult, therefore, because $b_5$ content is based on spectral analysis of its heme. In some experiments with glutathione reductase [30, 67,69], enzyme concentrations of 0.2 to 0.5 mg per ml (1.7 to 4.2 μM) were used. These are 9- to 22-fold greater than the molar $b_5$ concentration in our experiments (0.19 μM). The strong signals for DEPMPO adducts in our studies are therefore not the result of excess enzyme, but are indicative of the robust activity of these proteoliposomes to reduce Cr(VI) and generate ROS under Cr(VI)-reducing conditions.

Another noteworthy aspect of the findings here is that the proteoliposome system must generate sufficient $H_2O_2$ to support hydroxyl radical generation. This is in contrast to studies with chemical Cr(VI) reductants (e.g. ascorbate, glutathione, NADPH, cysteine) for which high concentrations (1 to 5 mM) of exogenous $H_2O_2$ have typically been added [27,29,34,66]. Cr (VI) reduction by α-lipoic acid is an exception to these studies in that hydroxyl radical was detected without adding $H_2O_2$ [25]. Similarly, Cr(VI) reduction by glutathione reductase can generate hydroxyl radical without the addition of $H_2O_2$ [26,28,30,67]. For both lipoic acid and glutathione reductase, catalase significantly diminished hydroxyl radical generation indicating that $H_2O_2$ was required [25,26,28,69]. The effects of catalase were similar in our proteoliposome studies, and indicate that Fenton-like reactions between partially reduced Cr species and $H_2O_2$ were responsible for the generation of hydroxyl radical.

With glutathione reductase, hydroxyl radical production coincident with Cr(VI) reduction is decreased significantly under anaerobic conditions indicating that $O_2$ is required [69]. We similarly noted a marked decline in hydroxyl radical signal with our proteoliposomes under anaerobic conditions. It was proposed that glutathione reductase simultaneously reduces Cr (VI) to Cr(V) and $O_2$ to $O_2^{\bullet -}$, and that the $O_2^{\bullet -}$ dismutates to $H_2O_2$ [69]. It is possible that a similar situation occurs with the proteoliposomes because we observed both $O_2^{\bullet -}$ and $HO^{\bullet}$ adducts of DEPMPO during Cr(VI) reduction under room air. While small amounts of $O_2^{\bullet -}$ were generated by proteoliposomes in the absence of Cr(VI), more $O_2^{\bullet -}$ was generated in the presence of Cr(VI) suggesting that Cr(VI) may stimulate $O_2$ reduction by the PLs. This would be similar to the situation with glutathione reductase [69]. Even in the absence of Cr(VI), microsomes are capable of generating superoxide and $H_2O_2$ [70].

In the proteoliposome studies, it is unlikely that Cr(V) is responsible for reducing $O_2$ to $O_2^{\bullet -}$. In fact, the opposite has been reported, i.e. that $O_2^{\bullet -}$ is capable of reducing Cr(VI) to Cr (V) [23,71]. However, it is unlikely that $O_2^{\bullet -}$ accounts for a significant percentage of Cr(VI) reduction in our system. First, SOD did not inhibit Cr(VI) reduction or the levels of DEPMPO/$^{\bullet}$OH adducts. Second, the PLs reduce Cr(VI) under anaerobic conditions in which minimal $O_2^{\bullet -}$ is generated.

The DEPMPO/$^{\bullet}$OH signals under aerobic conditions with the PLs reflect trapping of hydroxyl radical and are not confounded by direct reaction with Cr(V). The ability to simultaneously detect both superoxide and hydroxyl radical was noted, as were the pronounced signal intensities for the DEPMPO adducts relative to other Cr(VI) reduction studies which primarily used DMPO. This could reflect the robust activity of the proteoliposomes, but there are likely additional contributing factors that result from the advantageous properties of DEPMPO. In addition to the advantages noted above, significantly lower concentrations of DEPMPO are sufficient to detect adducts as compared with DMPO [51]. The reaction rate constants of DEPMPO with superoxide and hydroxyl radical are 1.5- and 2-fold, respectively, of those observed with DMPO [50]. In addition, DEPMPO can trap and stabilize hydroxyl radical as DEPMPO/$^{\bullet}$OH and superoxide as DEPMPO/OOH, giving ESR spectra characteristic of each [49]. While portions of their spectra overlap, the unique components of each provided for concurrent observation of both adducts. This is in contrast to studies with GSH reductase and

DMPO in which the DMPO/OOH adduct could only be observed if deferoxamine was included to chelate Cr(V) [69].

The proteoliposome studies here demonstrated that the redox cycling of Cr can result in a molar excess of $HO^{\bullet}$ relative to the net amount of Cr(VI) reduced (Fig. 9). While predicted in theory, we are not aware of other studies which have addressed this quantitatively over time with other Cr(VI) reductants. This stoichiometric excess is most apparent at the early time points and is enhanced by the addition of exogenous $H_2O_2$. This implies that, at early time points, hydroxyl radical generation is limited by the amount of $H_2O_2$ generated by the system, and not by the Cr(VI) reduction rate. The stoichiometric excess was not apparent at later times, however. When $H_2O_2$ is not added, it is possible that $H_2O_2$ production by the PLs becomes even more limiting at later times. This does not, however, explain the leveling off of DEPMPO/OH adducts at later times in those experiments in which $H_2O_2$ was added. It is possible that, at these later times, a larger percentage of the total Cr is further reduced to forms which cannot significantly contribute to continued $HO^{\bullet}$ generation. Since Cr(IV) can also mediate $HO^{\bullet}$ production [27,72], Cr(III) might predominate at these later times. Even though the superoxide and hydroxyl radical adducts do not continue to increase at later times, it is likely that both of these ROS continue to be produced at some level throughout these one hour experiments. The in vitro half-lives for the DEPMPO/OOH and DEPMPO/$^{\bullet}$OH adducts are 14.8 and 22.3 min, respectively [49,73]. If production of these ROS ceased once the maximal intensity of the adduct signals had been reached, there certainly would have been a noticeable decline in their signals at the later times. The relatively constant signal intensities at the later time points therefore suggest a continued rate of production sufficient to offset expected declines from their in vitro $t_{1/2}$.

Since spin trapping is never 100% efficient, the levels of DEPMPO/$^{\bullet}$OH and DEPMPO/OOH in Fig. 9 are no doubt underestimates. One study noted an efficiency of 60–70% for trapping superoxide [50]. Our observations suggested an efficiency of about 50% in that we noted a 2.1-fold increase in DEPMPO/OOH signal intensity when the spin trap concentration was increased from 14 mM to 500 mM. We observed an even lower efficiency (approx. 35%) for trapping $HO^{\bullet}$ with 14 mM DEPMPO. While too costly for routine use, the 500 mM DEPMPO results indicate that the levels of $HO^{\bullet}$ in Fig. 9 are underestimated by 2.8-fold. This suggests that the stoichiometric ratios for hydroxyl radical production vs. net Cr(VI) reduced (Fig. 9C) are similarly underestimated. If this 2.8-fold correction is applied to the ratios in Fig. 9C, then in the absence of added $H_2O_2$ there is a 7.7-fold excess of $HO^{\bullet}$ relative to net Cr(VI) reduced at the earliest time point and the ratio would remain above 1.0 for the first 15 min. When $H_2O_2$ was included, there would be a 17.7-fold excess of $HO^{\bullet}$ at the earliest time point and the ratio would remain above 1.0 for the entire hour. Given that even 500 mM DEPMPO may not be 100% efficient, the actual ratios could be higher still. In addition, some spin traps (e.g. DMPO), by trapping superoxide, can partially inhibit the dismutation of superoxide, thereby decreasing the available $H_2O_2$ to support hydroxyl radical generation [74]. SOD accelerates superoxide dismutation by $10^4$ [74]. For our experiments, simulation of the spectra indicated that SOD increased the DEPMPO/$^{\bullet}$OH adduct signal by 30% (Fig. 3D) when 14 mM DEPMPO was used. This increase might also result from protecting the DEPMPO/$^{\bullet}$OH adducts from reaction with superoxide which could convert them to ESR silent species [56,57]. Nonetheless, the data are consistent with a stoichiometric excess of $HO^{\bullet}$ generated relative to net Cr(VI) reduction. Such an excess could have significant implications for a free radical component to Cr toxicity.

Catalase is often used as one tool to determine if $H_2O_2$ is required for the formation of hydroxyl radical, including several studies with reactive Cr intermediates [25,26,28,75]. Examples of typical findings are that catalase decreases the intensity of the DMPO/OH signal while enhancing the Cr(V) signal [25,26] presumably because the removal of $H_2O_2$ prevents the

reoxidation of Cr(V) to Cr(VI). We noted similar observations in our preliminary experiments with proteoliposomes and catalase (Sigma C10) except that the enhancement of the Cr(V) signal was even larger than that for proteoliposomes under anaerobic conditions. It was subsequently discovered that some sources of catalase contain contaminants that reduce Cr (VI) in an NADPH-dependent manner, which would explain the larger than expected Cr(V) signals. Cr(VI) reduction is not an inherent property of catalase, however, so catalase devoid of this activity was used for the remainder of the experiments. Our ESR spectra with catalase, therefore, represent the effect of removal of $H_2O_2$ and are not complicated by Cr(VI) reductase activity in the catalase. The unexpected activity in some sources of catalase, however, underscores the need to screen catalase for possible interfering activities.

While iron is the classic metal associated with hydroxyl radical generation, there are several reasons why iron is not responsible for the bulk of hydroxyl radical generation in the studies reported here. First, the pretreatment of solutions with Chelex 100 resin should have removed transition metal contaminants. Second, it has previously been shown that iron contamination in this proteoliposome system is negligible [40]. Third, the vast majority of hydroxyl radical was generated only when NADPH, Cr(VI) and the proteoliposomes were all present. Little to no hydroxyl radical was detected when any one of these components was excluded (Fig. 3F, 4D,4E,4I,4J). Also, when the proteoliposome experiments were conducted in the presence of 0.1 mM diethylenetriaminepentaacetic acid (DTPA), the intensity of the DEPMPO/$^{\bullet}$OH signal decreased by only 34% (not shown); the DEPMPO/OOH signal concurrently increased such that the total amount of ROS ($HO^{\bullet} + O_2^{-\bullet}$) was essentially the same in the presence and absence of DTPA. The partial inhibitory effect of DTPA on $HO^{\bullet}$ generation is likely due to partial chelation of Cr species and is consistent with other reports, e.g. DTPA caused a partial decline in $HO^{\bullet}$ generation associated with Cr(VI) reduction by α-lipoic acid [25], and DTPA reduced the Cr(V) signal intensity by 31% in rodent studies [76]. In contrast to the effects of DTPA, deferoxamine (DFX) casued a much larger decline in the levels of DEPMPO/$^{\bullet}$OH adducts (Fig. 6). DFX also eliminated the vast majority of the Cr(V) ESR signal consistent with its ability to bind Cr(V) in other systems and largely diminish the Cr(V) ESR signal [30]. These results imply that Cr(V) has a significant role in the generation of hydroxyl radical by the proteoliposomes. This role could be direct via Cr(V)-mediated Fenton-like reactions, or it could be indirect as a precursor to Cr(IV), which also participates in Fenton-like reactions. However, the observation that catalase results in a large increase in the Cr(V) signal (Fig. 7E) implies that Cr(V) plays a significant role in generating hydroxyl radical in this system.

The phosphatidylcholine used to make the PLs contains 100% saturated fatty acids so there should not have been free radical-mediated lipid peroxidation reactions that are characteristic of unsaturated fatty acids [77].

In addition to the ability of Cr(V) and Cr(IV) to react directly with cell components such as lipids and DNA [34,65,78], the generation of hydroxyl radical by Fenton-type reactions of the partially reduced Cr species could also contribute to Cr(VI) toxicity. This could be especially true for lung epithelial cells in which $O_2$ tensions are consistently high. Not only do human microsomal enzymes reduce Cr(VI) to Cr(V) and Cr(IV) [39,40], they are also able to generate superoxide and $H_2O_2$ [70]. The generation of both reactive oxygen species and reactive Cr intermediates by microsomal enzymes could have important implications for hydroxyl radical formation in the vicinity of the SER in cells. Since the SER is physically contiguous with the nuclear membrane and SER enzymes are present within the nuclear membrane [79,80], the reactive Cr and oxygen species generated by microsomal enzymes could therefore have important implications for potential damage to DNA and the nuclear membrane.

These studies represent the robust in vitro activity of human cytochrome $b_5$ with regards to the reductive activation of Cr(VI) and the resulting generation of hydroxyl radical. The in vivo

contribution of cytochrome $b_5$ to this process remains to be determined. Since there are key differences between humans and rodents with respect to microsomal Cr(VI) reduction [36, 37], rodent studies cannot be used to assess its role in humans. However, several observations are consistent with a potential role for human $b_5$ in vivo. In the proteoliposomes used here, Cr (VI) reduction by $b_5$ is dependent on electrons from NADPH via P450 reductase. In human microsomes, cytochrome $b_5$ has a central role in Cr(VI) reduction which is dependent on either NADPH or NADH via P450 reductase or $b_5$ reductase, respectively [36,39]. This dependence is consistent with data from animals and cell lines which suggest that NAD(P)H-dependent enzymes are significant contributors to the 1-electron reduction of Cr(VI) in vivo [22,76,81, 82]. Cr(VI)-exposed human A549 cells (human lung epithelial cancer) generate DMPO/$^{\bullet}$OH adducts, and these adducts are increased by adding NADPH and decreased by catalase [75, 83,84]. NADPH also increases Cr(VI)-induced apoptosis in these cells [83]. NADPH increases the DMPO/$^{\bullet}$OH adducts in Cr(VI)-exposed murine macrophages [85].

Cr(VI) exposure is known to induce oxidant stress in vivo [86], and cytochrome $b_5$ is able to generate hydroxyl radical at low (10 μM) concentrations of Cr(VI). This is consistent with the kinetics of Cr(VI) reduction by human microsomes [36,37]. Cr(VI) treatment (10 μM) of A549 cells results in DNA strand breaks that involve DNA base oxidation as well as elevated 8-oxodeoxyguanosine levels [87]. Cr(VI) (10 μM) also increases the DMPO/$^{\bullet}$OH signal in A549 cells, and this signal is largely abolished by SOD plus catalase [68]. The c-Jun N-terminal kinase (JNK) is selectively activated in A549 cells by 10 μM Cr(VI), and pre-exposure of cells to *N*-acetylcysteine prevents this activation [68]. This level of Cr(VI) is also sufficient to alter the expression of dozens of genes [88] and to induce apoptosis in BEAS-2B (normal human bronchial epithelial) cells [89], and it causes extensive cell death in primary human fibroblasts [90].

Inhalational exposure of Cr is of primary concern, and bronchial epithelial cells are directly exposed to inhaled Cr. Chromium-associated tumors initiate at bronchial bifurcations where particulate Cr is preferentially deposited [4,5]. Since room air inhibits only a minority of human microsomal Cr(VI) reduction [36], microsomal enzymes could contribute significantly to Cr (VI) reduction in the lung. The relative Cr(VI) reducing activities of human lung and liver microsomes are consistent with their relative contents of cytochrome $b_5$ and P450 reductase [36,39]. The contribution of microsomal enzymes to Cr(VI) reduction in cells could vary with their content of these enzymes. In human lung, these microsomal enzymes are confined primarily to bronchial and bronchiolar epithelial cells [46] which are directly exposed to inhaled Cr(VI). While cytochrome $b_5$ was not examined, intratracheal Cr(VI) causes a 2- to 3-fold increase in the expression of pulmonary microsomal enzymes, including $b_5$ reductase and P450 reductase [41], so the contribution of these enzymes could increase during chronic Cr exposure. Overall, the properties of human microsomal enzymes including $b_5$ are consistent with a potentially significant role in the reductive activation of Cr(VI) and hydroxyl radical generation at low Cr(VI) concentrations and in human cells. A further examination of their role in normal human bronchial epithelial cells is warranted.

In summary, the findings indicate that the vast majority of hydroxyl radical in this system is generated as a consequence of the NADPH-dependent reduction of Cr(VI) by the proteoliposomes. This system generates superoxide and hydroxyl radical even at low μM Cr (VI) concentrations. Hydrogen peroxide was required for hydroxyl radical formation, but it did not have to be added indicating that sufficient amounts were generated by the proteoliposomes. Especially for the early time points, an excess of hydroxyl radical was generated relative to the net amount of Cr(VI) reduced. These findings are the first report of a role for cytochrome $b_5$ in a process that generates hydroxyl radical. The location of these enzymes within the cell and their ability to simultaneously generate both Cr(V) and $H_2O_2$ could have important implications for cellular Cr(VI) toxicity.

**Acknowledgements**

This project was supported by grant number ES012707 from the National Institute of Environmental Health Sciences (NIEHS), NIH. Its contents are solely the responsibility of the authors and do not necessarily represent the official views of the NIEHS, NIH.

The EPR facilities of the Department of Biophysics are supported by National Biomedical ESR Center Grant EB001980 from the NIH.

We are grateful to Dr. Neil Hogg for his assistance with the Winsim EPR simulation software, and to Dr. David H. Petering for kindly supplying the $Na_2{}^{53}CrO_4$.

This project was supported by National Institutes of Health grant 5R01ES012707.

## References

1. Taioli E, Zhitkovich A, Kinney P, Udasin I, Toniolo P, Costa M. Increased DNA-protein crosslinks in lymphocytes of residents living in chromium-contaminated areas. Biol Trace Elem Res 1995;50:175–180. [PubMed: 8962789]
2. Costa M, Zhitkovich A, Toniolo P, Taioli E, Popov T, Lukanova A. Monitoring human lymphocytic DNA-protein cross-links as biomarkers of biologically active doses of chromate. Environ Health Perspect 1996;104:917–919. [PubMed: 8933034]
3. Raithel H-J, Schaller K-H, Kraus T, Lehnert G. Biomonitoring of nickel and chromium in human pulmonary tissue. Int Arch Occup Environ Health 1993;65:S197–S200. [PubMed: 8406925]
4. Ishikawa Y, Nakagawa K, Satoh Y, Kitagawa T, Sugano H, Hirano T, Tsuchiya E. “Hot spots” of chromium accumulation at bifurcations of chromate workers' bronchi. Cancer Res 1994;54:2343–2346.
5. Ishikawa Y, Nakagawa K, Satoh Y, Kitagawa T, Sugano H, Hirano T, Tsuchiya E. Characteristics of chromate workers' cancers, chromium lung deposition and precancerous bronchial lesions: an autopsy study. Br J Cancer 1994;70:160–166. [PubMed: 8018529]
6. Hayes, RB. Carcinogenic effects of chromium. In: Langard, S., editor. Biological and Environmental Aspects of Chromium. 5. Amsterdam: Elsevier Biomedical Press; 1982. p. 221-239.
7. Deschamps F, Moulin JJ, Wild P, Labriffe H, Haguenoer JM. Mortality study among workers producing chromate pigments in France. Int Arch Occup Environ Health 1995;67:147–152. [PubMed: 7591171]
8. Langard S. Role of chemical species and exposure characteristics in cancer among persons occupationally exposed to chromium compounds. Scand J Work Environ Health 1993;19(Suppl 1): 81–89. [PubMed: 8159981]
9. Gadd GM, White C. Microbial treatment of metal pollution — a working biotechnology? TIBTECH (August) 11:1993.
10. Environmental Protection Agency. Chromium. Integrated Risk Information System, Office of Health and Environmental Assessment; U.S. EPA: 1999.
11. Zhitkovich A, Voitkun V, Kluz T, Costa M. Utilization of DNA-protein cross-links as a biomarker of chromium exposure. Environ Health Perspect 1998;106(suppl 4):969–974. [PubMed: 9703480]
12. Kortenkamp A, Beyersmann D, O’Brien P. Uptake of chromium(III) complexes by erythrocytes. Toxicol Environ Chem 1987;14:23–32.
13. Baruthio F. Toxic effects of chromium and its compounds. Biol Trace Element Res 1992;32:145–153.
14. Buttner B, Beyersmann D. Modification of the erythrocyte anion carrier by chromate. Xenobiotica 1985;15:735–741. [PubMed: 4072261]
15. Cantoni O, Costa M. Analysis of the induction of alkali sensitive sites in the DNA by chromate and other agents that induce single strand breaks. Carcinogenesis 1984;5:1207–1209. [PubMed: 6467509]
16. Christie NT, Cantoni O, Evans RM, Meyn RE, Costa M. Use of mammalian DNA repair-deficient mutants to assess the effects of toxic metal compounds on DNA. Biochem Pharmacol 1984;33:1661–1670. [PubMed: 6233980]

17. Levy LS, Venitt S. Carcinogenicity and mutagenicity of chromium compounds: the association between bronchial metaplasia and neoplasia. Carcinogenesis 1986;7:831–835. [PubMed: 3698209]
18. Tsapakos MJ, Hampton TH, Wetterhahn KE. Chromium(VI)-induced DNA lesions and chromium distribution on rat kidney, liver and lung. Cancer Res 1983;43:5662–5667. [PubMed: 6640521]
19. Whiting RF, Stich HF, Koropatnick DJ. DNA damage and DNA repair in cultured human cells exposed to chromate. Chem-Biol Interactions 1979;26:267–280.
20. Standeven AM, Wetterhahn KE. Is there a role for reactive oxygen species in the mechanism of chromium(VI) carcinogenesis? Chem Res Toxicol 1991;4:616–625. [PubMed: 1807444]
21. Dillon CT, Lay PA, Bonin AM, Cholewa M, Legge GJF, Collins TJ, Kostka KL. Permeability, cytotoxicity, and genotoxicity of chromium(V) and chromium(VI) complexes in V79 Chinese hamster lung cells. Chem Res Toxicol 1998;11:119–129. [PubMed: 9511903]
22. Shi X, Chiu A, Chen CT, Halliwell B, Castranova V, Vallyathan V. Reduction of chromium(VI) and its relationship to carcinogenesis. J Toxicol Environ Health, Pt B 1999;2: 87–104.
23. Shi X, Dalal NS. The role of superoxide radical in chromium(VI)-generated hydroxyl radical: the Cr (VI) Haber-Weiss cycle. Arch Biochem Biophys 1992;292:323–327. [PubMed: 1309299]
24. Shi X, Ding M, Ye J, Wang S, Leonard SS, Zang L, Castranova V, Vallyathan V, Chiu A, Dalal N, Liu K. Cr(IV) causes activation of nuclear transcription factor-κB, DNA strand breaks and dG hydroxylation via free radical reactions. J Inorg Biochem 1999;75:37–44. [PubMed: 10402675]
25. Chen F, Ye J, Zhang X, Rojanasakul Y, Shi X. One-electron reduction of chromium(VI) by alpha-lipoic acid and related hydroxyl radical generation, dG hydroxylation and nuclear transcription factor-kappaB activation. Arch Biochem Biophys 1997;338:165–72. [PubMed: 9028868]
26. Shi X, Dalal NS. NADPH-dependent flavoenzymes catalyze one electron reduction of metal ions and molecular oxygen and generate hydroxyl radicals. FEBS Lett 1990;276:189–191. [PubMed: 2176163]
27. Shi X, Mao Y, Knapton AD, Ding M, Rojanasakul Y, Gannett PM, Dalal N, Liu K. Reaction of Cr (VI) with ascorbate and hydrogen peroxide generates hydroxyl radicals and causes DNA damage: role of a Cr(IV)-mediated Fenton-like reaction. Carcinogenesis 1994;15:2475–2478. [PubMed: 7955094]
28. Shi XL, Dalal NS. One-electron reduction of chromate by NADPH-dependent glutathione reductase. J Inorg Biochem 1990;40:1–12. [PubMed: 2178178]
29. Shi XL, Dalal NS. ESR spin trapping detection of hydroxyl radicals in the reactions of Cr(V) complexes with hydrogen peroxide. Free Radic Res Commun 1990;10:17–26. [PubMed: 2165982]
30. Shi X, Sun X, Gannett PM, Dalal NS. Deferoxamine inhibition of Cr(V)-mediated radical generation and deoxyguanine hydroxylation: ESR and HPLC evidence. Arch Biochem Biophys 1992;293:281–286. [PubMed: 1311164]
31. Standeven AM, Wetterhahn KE. Ascorbate is the principal reductant of chromium(VI) in rat lung ultrafiltrates and cytosols, and mediates chromium-DNA binding *in vitro*. Carcinogenesis 1992;13:1319–1324. [PubMed: 1499083]
32. Mikalsen A, Alexander J, Ryberg D. Microsomal metabolism of hexavalent chromium. Inhibitory effect of oxygen and involvement of cytochrome P-450. Chem-Biol Interact 1989;69:175–192. [PubMed: 2495190]
33. Jennette KW. Microsomal reduction of the carcinogen chromate produces chromium(V). J Am Chem Soc 1982;104:874–875.
34. Shi X, Dong Z, Dalal NS, Gannett PM. Chromate-mediated free radical generation from cysteine, penicillamine, hydrogen peroxide, and lipid hydroperoxides. Biochim Biophys Acta 1994;1226:65–72. [PubMed: 8155741]
35. Suzuki Y, Fukuda K. Reduction of hexavalent chromium by ascorbic acid and glutathione with special reference to the rat lung. Arch Toxicol 1990;64:169–176. [PubMed: 2372230]
36. Myers CR, Myers JM. Iron stimulates the rate of reduction of hexavalent chromium by human microsomes. Carcinogenesis 1998;19:1029–1038. [PubMed: 9667741]
37. Pratt PF, Myers CR. Enzymatic reduction of chromium(VI) by human hepatic microsomes. Carcinogenesis 1993;14:2051–2057. [PubMed: 8222053]
38. Myers CR, Porgilsson B, Carstens BP, Myers JM. Naphthoquinones stimulate the rate of reduction of hexavalent chromium by human microsomes. Toxic Subst Mech 1999;18:103–128.

39. Myers CR, Myers JM, Carstens BP, Antholine WE. Reduction of chromium(VI) to chromium(V) by human microsomal enzymes: effects of iron and quinones. Toxic Subst Mech 2000;19:25–51.
40. Jannetto PJ, Antholine WE, Myers CR. Cytochrome $b_5$ plays a key role in human microsomal chromium(VI) reduction. Toxicology 2001;159:119–133. [PubMed: 11223168]
41. Izzotti A, Cartiglia C, Balansky R, D'Agostini F, Longobardi M, De Flora S. Selective induction of gene expression in rat lung by hexavalent chromium. Mol Carcinogenesis 2002;35:75–84.
42. Nakagawa K, Matsubara T, Kinoshita I, Tsuchiya E, Sugano H, Hirano T. Surveillance study of a group of chromate workers — early detection and high incidence of lung cancer (in Japanese). Lung Cancer 1984;24:301–310.
43. Becker N, Chang-Claude J, Frentzel-Beyme R. Risk of cancer for arc welders in the Federal Republic of Germany: results of a second follow up (1983–8). Br J Ind Med 1991;48:675–683. [PubMed: 1931726]
44. Franchini I, Magnani F, Mutti A. Mortality experience among chromplating workers. Scand J Work Environ Health 1983;9:247–252. [PubMed: 6612265]
45. Stern RM. Assessment of risk of lung cancer for welders. Arch Environ Health 1983;38:148–155. [PubMed: 6347098]
46. Hall Pde la M, Stupans I, Burgess W, Birkett DJ, McManus ME. Immunohistochemical localization of NADPH-cytochrome P450 reductase in human tissues. Carcinogenesis 1989;10:521–530. [PubMed: 2493999]
47. Ingelman-Sundberg M, Glaumann H. Incorporation of purified components of the rabbit liver microsomal hydroxylase system into phospholipid vesicles. Biochim Biophys Acta 1980;599:417–435. [PubMed: 6773567]
48. Kajihara T, Hagihara B. Crystalline cytochrome $b_5$. I. Purification of crystalline cytochromes $b_5$ from rabbit liver. J Biochem (Tokyo) 1968;63:453–461. [PubMed: 5724556]
49. Frejaville C, Karoui H, Tuccio B, Le Moigne F, Culcasi M, Pietri S, Lauricella R, Tordo P. 5-(Diethoxyphosphoryl)-5-methyl-1-pyrroline *N*-oxide: a new efficient phosphorylated nitrone for the in vitro and in vivo spin trapping of oxygen-centered radicals. J Med Chem 1995;38:258–265. [PubMed: 7830268]
50. Tordo, P. Spin-trapping: recent developments and applications. In: Gilbert, BC.; Atherton, NM.; Davies, MJ., editors. Electron Paramagnetic Resonance Specialist Periodical Reports. 16. Cambridge: The Royal Society of Chemistry; 1998. p. 116-144.
51. Liu KJ, Miyake M, Panz T, Swartz H. Evaluation of DEPMPO as a spin trapping agent in biological systems. Free Radic Biol Med 1999;26:714–721. [PubMed: 10218661]
52. Duling DR. Simulation of multiple isotropic spin-trap EPR spectra. J Magn Reson B 1994;104:105–110. [PubMed: 8049862]
53. Stearns DM, Wetterhahn KE. Reaction of chromium(VI) with ascorbate produces chromium(V), chromium(IV), and carbon-based radicals. Chem Res Toxicol 1994;7:219–230. [PubMed: 8199312]
54. Molyneux MJ, Davies MJ. Direct evidence for hydroxyl radical-induced damage to nucleic acids by chromium(VI)-derived species. Carcinogenesis 1995;16:875–882. [PubMed: 7537182]
55. Vásquez-Vivar J, Hogg N, Martásek P, Karoui H, Tordo P, Pritchard KAJ, Kalyanaraman B. Effect of redox-active drugs on superoxide generation from nitric oxide synthases: biological and toxicological implications. Free Radic Res 1999;31:607–617. [PubMed: 10630684]
56. Reinke LA, Moore DR, McCay PB. Degradation of DMPO adducts from hydroxyl and 1-hydroxyethyl radicals by rat liver microsomes. Free Radic Res 1996;25:467–474. [PubMed: 8951420]
57. Kosaka H, Katsuki Y, Shiga T. Spin trapping study on the kinetics of $Fe^{2+}$ autoxidation: formation of spin adducts and their destruction by superoxide. Arch Biochem Biophys 1992;293:401–408. [PubMed: 1311166]
58. Karoui H, Hogg N, Fréjaville C, Tordo P, Kalyanaraman B. Characterization of sulfur-centered radical intermediates formed during the oxidation of thiols and sulfite by peroxynitrite. J Biol Chem 1996;271:6000–6009. [PubMed: 8626383]
59. Sugden KD, Wetterhahn KE. Reaction of chromium(V) with the EPR spin traps 5,5-dimethylpyrroline *N*-oxide and phenyl-*N*-*tert*-butylnitrone resulting in direct oxidation. Inorg Chem 1996;35:651–657.

60. Kotake Y, Janzen EG. Decay and fate of the hydroxyl radical adduct of α-phenyl-*N*-*tert*-butylnitrone in aqueous media. J Am Chem Soc 1991;113:9503–9506.
61. Janzen EG, Kotake Y, Hinton RD. Stabilities of hydroxyl radical spin adducts of PBN-type spin traps. Free Radic Biol Med 1992;12:169–173. [PubMed: 1313775]
62. Britigan BE, Coffman TJ, Buettner GR. Spin trapping evidence for the lack of significant hydroxyl radical production during the respiration burst of human phagocytes using a spin adduct resistant to superoxide-mediated destruction. J Biol Chem 1990;265:2650–2656. [PubMed: 2154454]
63. Burkitt MJ, Mason RP. Direct evidence for in vivo hydroxyl-radical generation in experimental iron overload: an ESR spin-trapping investigation. Proc Natl Acad Sci USA 1991;88:8440–8444. [PubMed: 1656444]
64. Perkins, MJ. Spin trapping. In: Gold, V.; Bethel, D., editors. Advances in Physical Organic Chemistry. 17. New York: Academic Press; 1980. p. 1-64.
65. Sugden KD, Campo CK, Martin BD. Direct oxidation of guanine and 7,8-dihydro-8-oxoguanine in DNA by a high-valent chromium complex: a possible mechanism for chromate genotoxicity. Chem Res Toxicol 2001;14:1315–1322. [PubMed: 11559048]
66. Shi X, Dalal NS. On the hydroxyl radical formation in the reaction between hydrogen peroxide and biologically generated chromium(V) species. Arch Biochem Biophys 1990;277:342–350. [PubMed: 2155579]
67. Leonard SS, Vallyathan V, Castranova V, Shi X. Generation of reactive oxygen species in the enzymatic reduction of $PbCrO_4$ and related DNA damage. Mol Cell Biochem 2002;234–235:309–315.
68. O'Hara KA, Klei LR, Barchowsky A. Selective activation of Src family kinases and JNK by low levels of chromium(VI). Toxicol Appl Pharmacol 2003;190:214–223. [PubMed: 12902192]
69. Leonard S, Wang S, Zang L, Castranova V, Vallyathan V, Shi X. Role of molecular oxygen in the generation of hydroxyl and superoxide anion radicals during enzymatic Cr(VI) reduction and its implication to Cr(VI)-induced carcinogenesis. J Environ Pathol Toxicol Oncol 2000;19:49–60. [PubMed: 10905508]
70. Rashba-Step J, Cederbaum AI. Generation of reactive oxygen intermediates by human liver microsomes in the presence of NADPH or NADH. Mol Pharmacol 1994;45:150–157. [PubMed: 8302274]
71. Shi X, Leonard SS, Zang L, Gannett P, Rojanasakul Y, Castranova V, Vallyathan V. Cr(III)-mediated hydroxyl radical generation via Haber-Weiss cycle. J Inorg Biochem 1998;69:263–268.
72. Luo H, Lu Y, Shi X, Mao Y, Dalal NS. Chromium(IV)-mediated Fenton-like reaction causes DNA damage: implication to genotoxicity of chromate. Ann Clin Lab Sci 1996;26:185–191. [PubMed: 8852428]
73. Khan N, Wilmot CM, Rosen GM, Demidenko E, Sun J, Joseph J, O'Hara J, Kalyanaraman B, Swartz HM. Spin traps: in vitro toxicity and stability of radical adducts. Free Radic Biol Med 2003;34:1473–1481. [PubMed: 12757857]
74. Britigan BE, Roeder TL, Buettner GR. Spin traps inhibit formation of hydrogen peroxide via the dismutation of superoxide: implications for spin trapping the hydroxyl free radical. Biochim Biophys Acta 1991;1075:213–222. [PubMed: 1659450]
75. Qian Y, Jiang BH, Flynn DC, Leonard SS, Wang S, Zhang Z, Ye J, Chen F, Wang L, Shi X. Cr (VI) increases tyrosine phosphorylation through reactive oxygen species-mediated reactions. Mol Cell Biochem 2001;222:199–204. [PubMed: 11678602]
76. Liu KJ, Shi X. In vivo reduction of chromium(VI) and its related free radical generation. Mol Cell Biochem 2001;222:41–47. [PubMed: 11678610]
77. Venkataraman S, Schafer FQ, Buettner GR. Detection of lipid radicals using EPR. Antioxid Redox Signal 2004;6:631–638. [PubMed: 15130290]
78. Mao Y, Zang L, Shi X. Generation of free radicals by Cr(IV) from lipid hydroperoxides and its inhibition by chelators. Biochem Mol Biol Int 1995;36:327–337. [PubMed: 7663436]
79. Moody DE, Clawson GA, Geller DA, Taylor LA, Button J, Loury DN, Hammock BD, Smuckler EA. Sodium cholate extraction of rat liver nuclear xenobiotic-metabolizing enzymes. Biochem Pharmacol 1988;37:1331–1341. [PubMed: 3128299]

80. Borgese N, Pietrini G. Distribution of the integral membrane protein NADH-cytochrome $b_5$ reductase in rat liver cells, studied with a quantitative radioimmunoblotting assay. Biochem J 1986;239:393–403. [PubMed: 3814080]

81. Liu KJ, Shi X. In vivo reduction of chromium (VI) and its related free radical generation. Mol Cell Biochem 2001;222:41–47. [PubMed: 11678610]

82. Liu K, Husler J, Ye J, Leonard SS, Cutler D, Chen F, Wang S, Zhang Z, Ding M, Wang L, Shi X. On the mechanism of Cr (VI)-induced carcinogenesis: dose dependence of uptake and cellular responses. Mol Cell Biochem 2001;222:221–229. [PubMed: 11678606]

83. Ye J, Wang S, Leonard SS, Sun Y, Butterworth L, Antonini J, Ding M, Rojanasakul Y, Vallyathan V, Castranova V, Shi X. Role of reactive oxygen species and p53 in chromium(VI)-induced apoptosis. J Biol Chem 1999;274:34974–34980. [PubMed: 10574974]

84. Wang S, Leonard SS, Ye J, Ding M, Shi X. The role of hydroxyl radical as a messenger in Cr(VI)-induced p53 activation. Am J Physiol - Cell Physiol 2000;279:C868–C875. [PubMed: 10942736]

85. Leonard SS, Roberts JR, Antonini JM, Castranova V, Shi X. $PbCrO_4$ mediates cellular responses via reactive oxygen species. Mol Cell Biochem 2004;255:171–179. [PubMed: 14971658]

86. Kadiiska MB, Morrow JD, Awad JA, Roberts LJ II, Mason RP. Identification of free radical formation and $F_2$-isoprostanes in vivo by acute Cr(VI) poisoning. Chem Res Toxicol 1998;11:1516–1520. [PubMed: 9860496]

87. Hodges NJ, Adam B, Lee AJ, Cross HJ, Chipman JK. Induction of DNA-strand breaks in human peripheral blood lymphocytes and A549 lung cells by sodium dichromate: association with 8-oxo-2-deoxyguanosine formation and inter-individual variability. Mutagenesis 2001;16:467–474. [PubMed: 11682636]

88. Andrew AS, Warren AJ, Barchowsky A, Temple KA, Klei L, Soucy NV, O'Hara KA, Hamilton JW. Genomic and proteomic profiling of responses to toxic metals in human lung cells. Environ Health Perspect 2003;111:825–835. [PubMed: 12760830]

89. Gambelunghe A, Piccinini R, Abbritti G, Ambrogi M, Ugolini B, Marchetti C, Migliorati G, Balducci C, Muzi G. Chromium VI-induced apoptosis in a human bronchial epithelial cell line (BEAS-2B) and a lymphoblastic leukemia cell line (MOLT-4). J Occup Environ Med 2006;48:319–325. [PubMed: 16531837]

90. Wise JP Sr, Wise SS, Little JE. The cytotoxicity and genotoxicity of particulate and soluble hexavalent chromium in human lung cells. Mutat Res 2002;517:221–229. [PubMed: 12034323]

## Abbreviations

**DEPMPO**
5-Diethoxyphos-phoryl-5-methyl-1-pyrroline-*N*-oxide

**DFX**
deferoxamine

**DMPO**
5,5,-dimethylpyrroline *N*-oxide

**DMSO**
dimethylsulfoxide

**DTPA**
diethylenetriaminepentaacetic acid

**$HO^{\bullet}$**
hydroxyl radical

**$^{\bullet}CH_3$**
methyl radical

**$^{\bullet}OCH_3$**

methoxy radical

**PBN**
α-phenyl-*N*-*tert*-butylnitrone

**PMSF**
phenylmethylsulfonyl fluoride

**PLs**
proteoliposomes

**ROS**
reactive oxygen species

**SER**
smooth endoplasmic reticulum

**$O_2^{\bullet-}$**
superoxide

**SOD**
superoxide dismutase

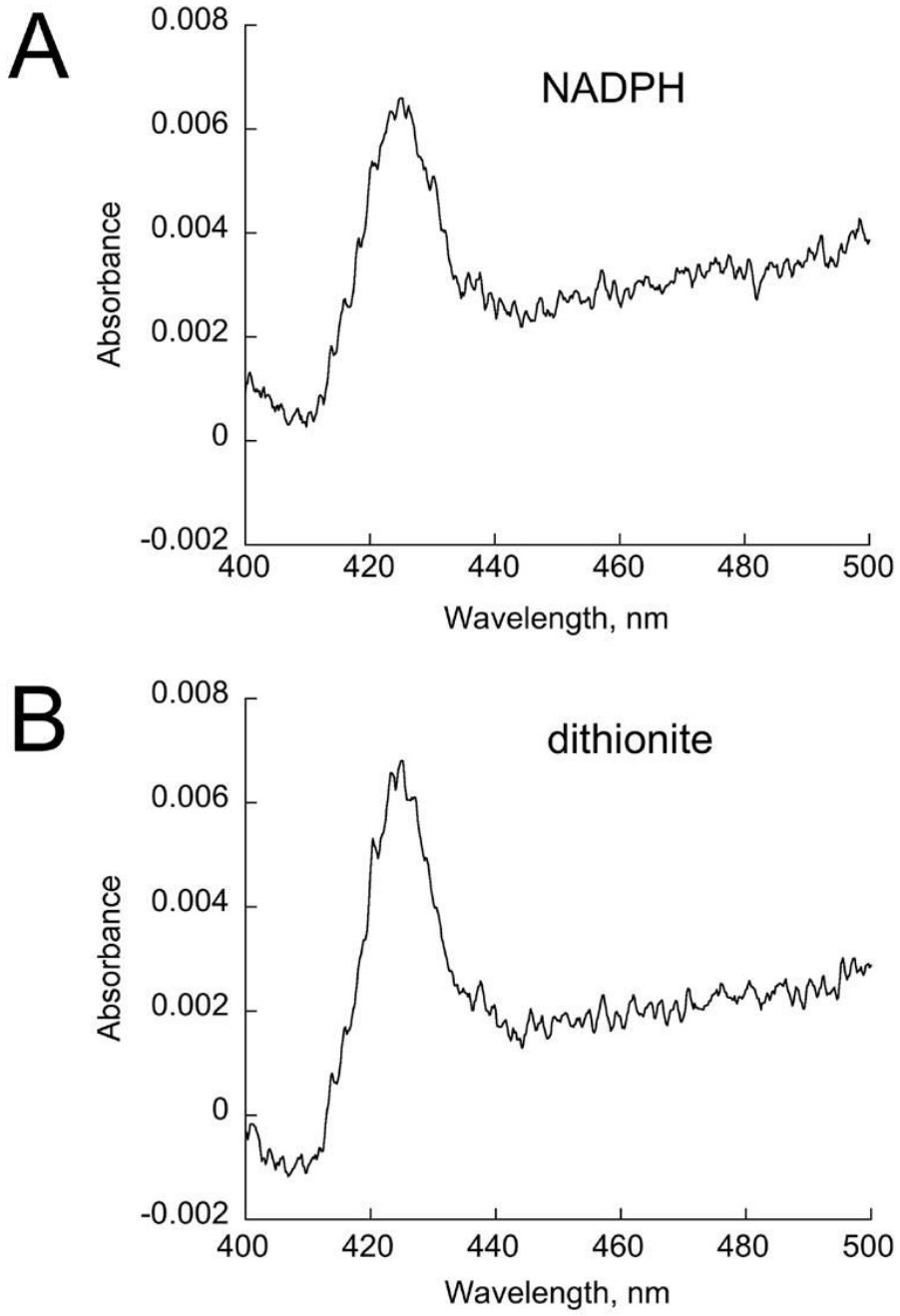


**Fig 1.**

Wavelength scans of reduced-minus-oxidized cytochrome $b_5$. (A) Reconstituted proteoliposomes containing P450 reductase and cytochrome $b_5$ after 6 min incubation at 37° C with 0.2 mM NADPH. (B) Sample A following the addition of an excess of sodium dithionite.

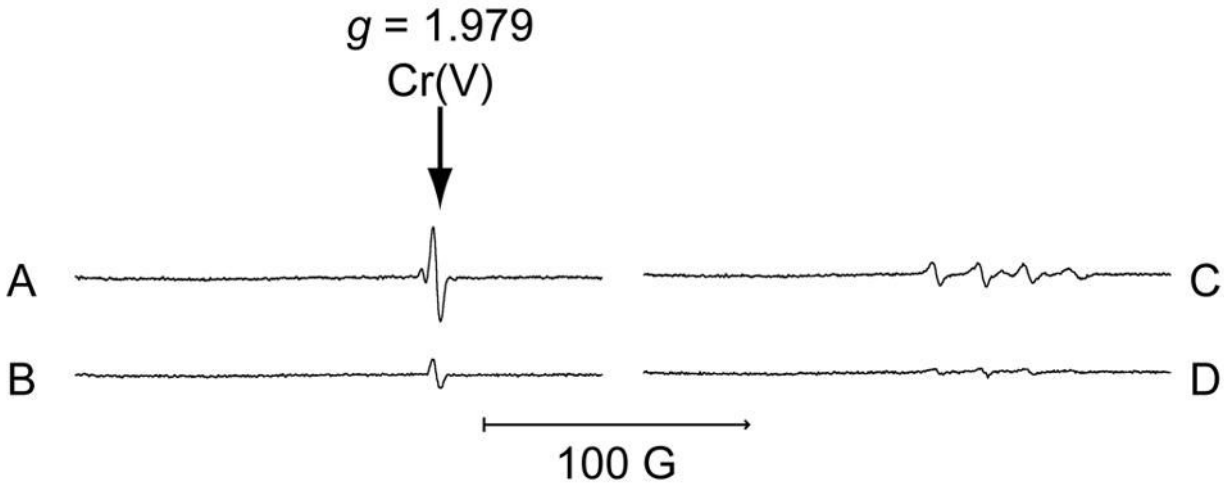


**Fig 2.**

ESR spectra of Cr(V) obtained during NADPH-dependent Cr(VI) reduction catalyzed by proteoliposomes containing cytochrome $b_5$ plus P450 reductase (10 min incubation at 37°C under room air). Samples included: (A) proteoliposomes plus 50 μM $Na_2CrO_4$ plus the NADPH-generating mix; (B) same as A but without liposomes; (C and D) same as A and B, respectively, except that $Na_2{}^{53}CrO_4$ was substituted for $Na_2CrO_4$. For each, the total reaction volume was 0.75 ml and the amount of proteoliposomes added contained 0.142 nmol cytochrome $b_5$. Instrument settings were as follows: 1 G modulation amplitude, 19.92 mW microwave power, 6.32 x $10^4$ receiver gain, 40.96 msec time constant, 9.76 GHz microwave frequency, sweep width = 200 G, field set = 3480 G, modulation frequency = 100 kHz, scan time = 42 sec; number of scans, 9. The results represent the average of two experiments.

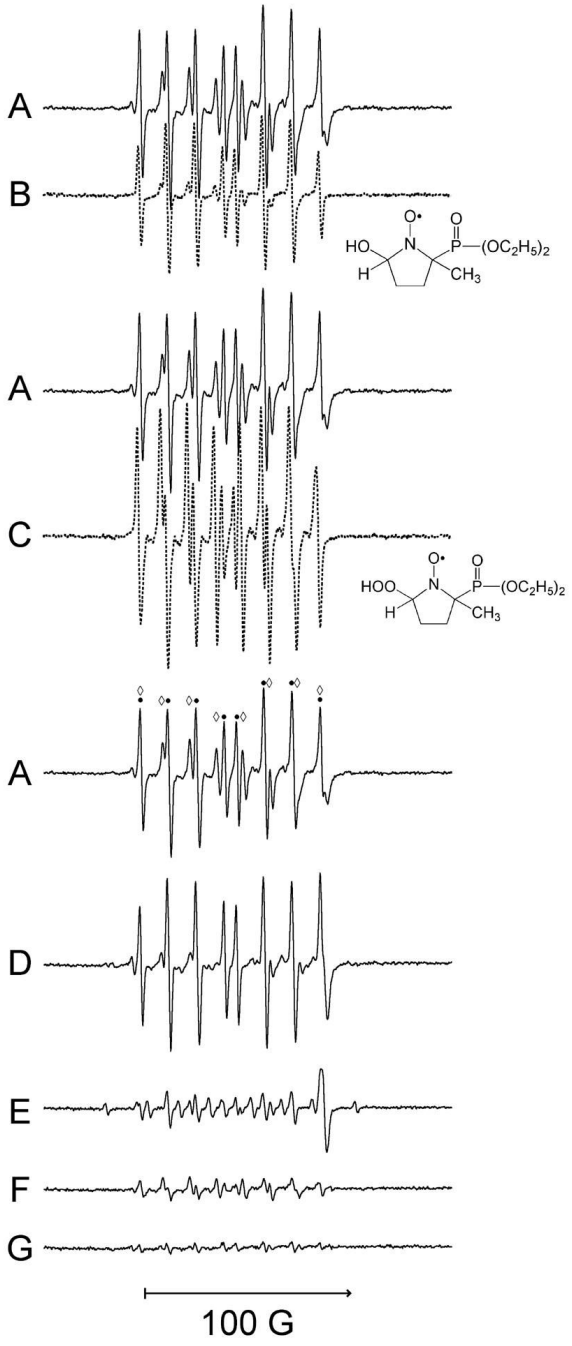


**Fig 3. ESR spectra obtained of aerobic reactions using the spin trap DEPMPO**

(A) NADPH-generating mix, 100 μM $Na_2CrO_4$, 14 mM DEPMPO, plus proteoliposomes containing cytochrome $b_5$ (0.0475 nmol) and P450 reductase in a total volume of 0.25 ml (10 min incubation at 37°C under room air). Note that the spectrum labeled A is shown three times to allow direct comparison to other signals. (B) hydroxyl radical positive control consisting of $H_2O_2$ (1.7 mM), ferrous ammonium sulfate (0.15 mM), and DEPMPO (14 mM) (10 min incubation at 37°C under room air). (C) superoxide positive control consisting of xanthine (2 mM), xanthine oxidase (0.2 units), DTPA (0.1 mM), DEPMPO (50 mM), and 50 mM potassium phosphate, pH 7.4, Chelex-treated, in a total volume of 0.25 ml (3 min incubation at 37°C under room air). The signals for the positive controls were offset vertically from that

of the proteoliposomes to facilitate comparison. The structures for the DEPMPO/•OH and DEPMPO/OOH adducts are shown next to traces B and C, respectively. For spectrum A shown alone, the signal correpsonding to DEPMPO/•OH is indicated by black dots above the spectrum, whereas that for DEPMPO/OOH is indicated by open diamonds. (D) Same as A plus 100 U SOD. (E) Same as A plus 100 U SOD and 550 U catalase (Sigma C100). (F) Same as A but without $Na_2CrO_4$. (G) Same as F plus 100 U SOD.
Instrument settings were as follows: 1 G modulation amplitude, 19.92 mW microwave power, $6.32 \times 10^4$ receiver gain, 40.96 msec time constant, 9.76 GHz microwave frequency, sweep width = 200 G, field set = 3480 G, modulation frequency = 100 kHz, scan time = 42 sec; number of scans, 9.

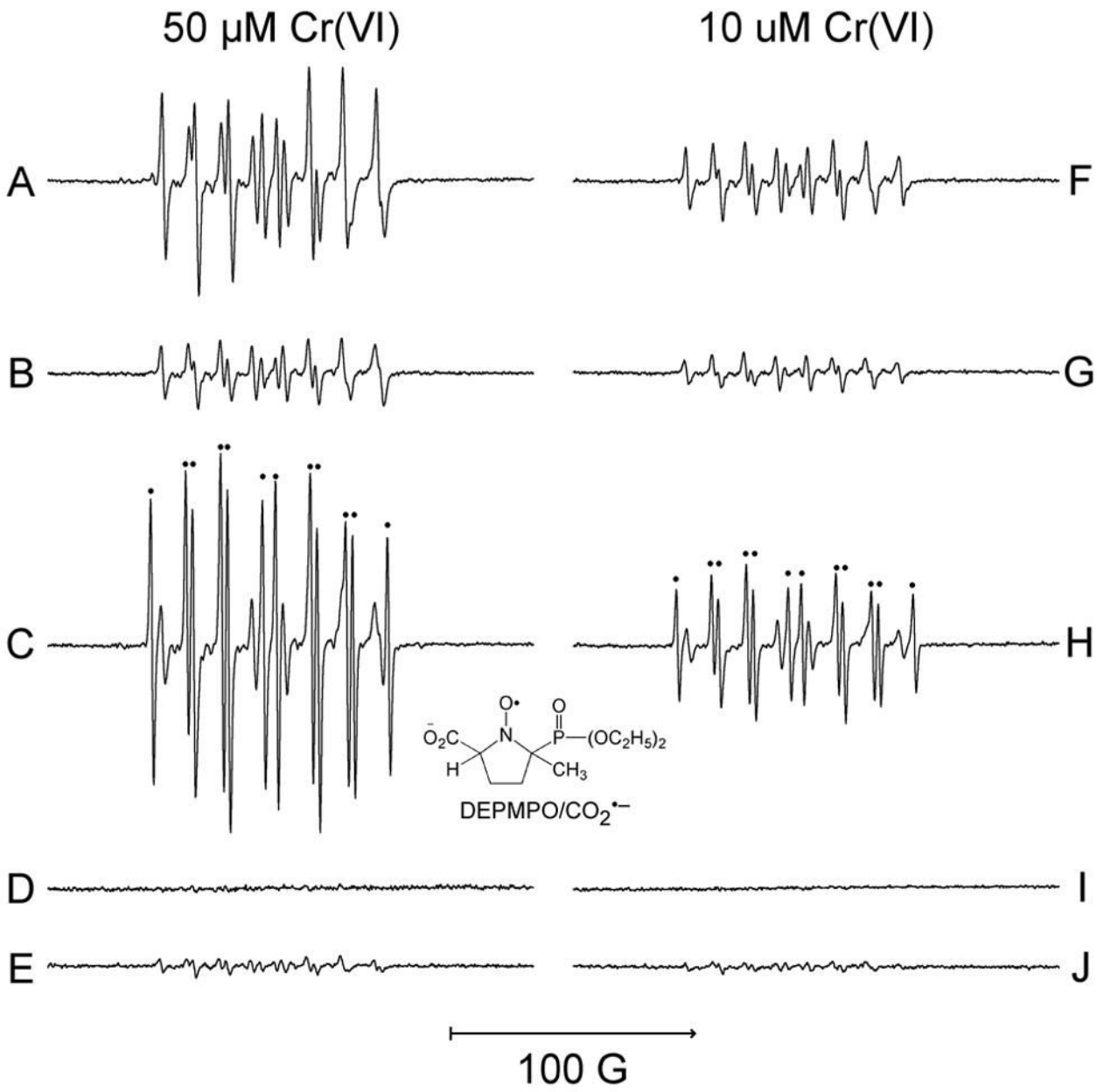


**Fig 4.**

ESR spectra obtained during the NADPH-dependent Cr(VI) reduction catalyzed by proteoliposomes containing cytochrome $b_5$ plus P450 reductase (10 min incubation at 37°C under room air). All samples included DEPMPO (14 mM) plus the following: (A) proteoliposomes plus 50 μM $Na_2CrO_4$ plus the NADPH-generating mix; (B) same as A plus catalase (550 U, Sigma C100); (C) same as A plus ammonium formate (250 mM); (D) same as A but without the NADPH-generating mix; (E) same as A but without the proteoliposomes. (F, G, H, I, and J) same as A, B, C, D, and E, respectively, except that the initial $Na_2CrO_4$ was 10 μM. For C and H, the structure of the DEPMPO/$CO_2^{\bullet -}$ adduct is shown, and the corresponding peaks are indicated with dots. For each, the total reaction volume was 0.25 ml and the amount of proteoliposomes added contained 0.0475 nmol cytochrome $b_5$. Instrument settings were as follows: 1 G modulation amplitude, 19.97 mW microwave power, 6.32 x

$10^4$ receiver gain, 40.96 msec time constant, 9.76 GHz microwave frequency, sweep width = 200 G, field set = 3480 G, modulation frequency = 100 kHz, scan time = 42 sec; number of scans, 9.

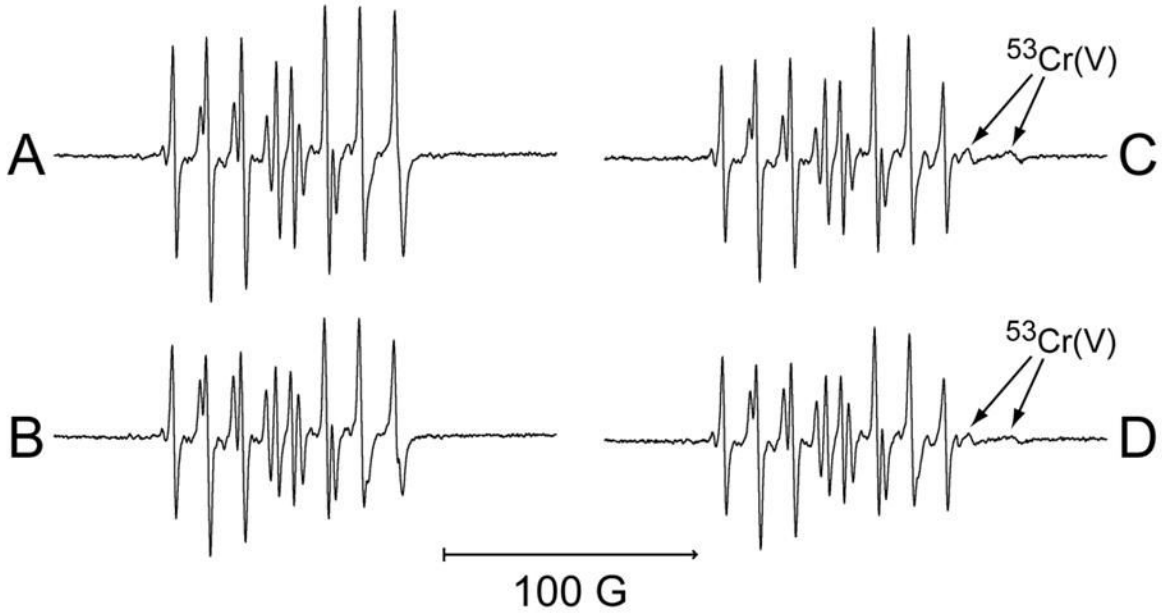


**Fig 5.**

ESR spectra obtained during the NADPH-dependent Cr(VI) reduction catalyzed by proteoliposomes containing cytochrome $b_5$ plus P450 reductase (10 min incubation at 37°C under room air). All samples included DEPMPO (14 mM) plus the following: (A) proteoliposomes plus 100 μM $Na_2CrO_4$ plus the NADPH-generating mix; (B) same as A except that initial $Na_2CrO_4$ was 50 μM; (C and D) same as A and B, respectively, except that $Na_2{}^{53}CrO_4$ was substituted for $Na_2CrO_4$. For each, the total reaction volume was 0.25 ml and the amount of proteoliposomes added contained 0.0475 nmol cytochrome $b_5$. Instrument settings were as follows: 1 G modulation amplitude, 19.97 mW microwave power, 6.32 x $10^4$ receiver gain, 40.96 msec time constant, 9.76 GHz microwave frequency, sweep width = 200 G, field set = 3480 G, modulation frequency = 100 kHz, scan time = 42 sec; number of scans, 9.

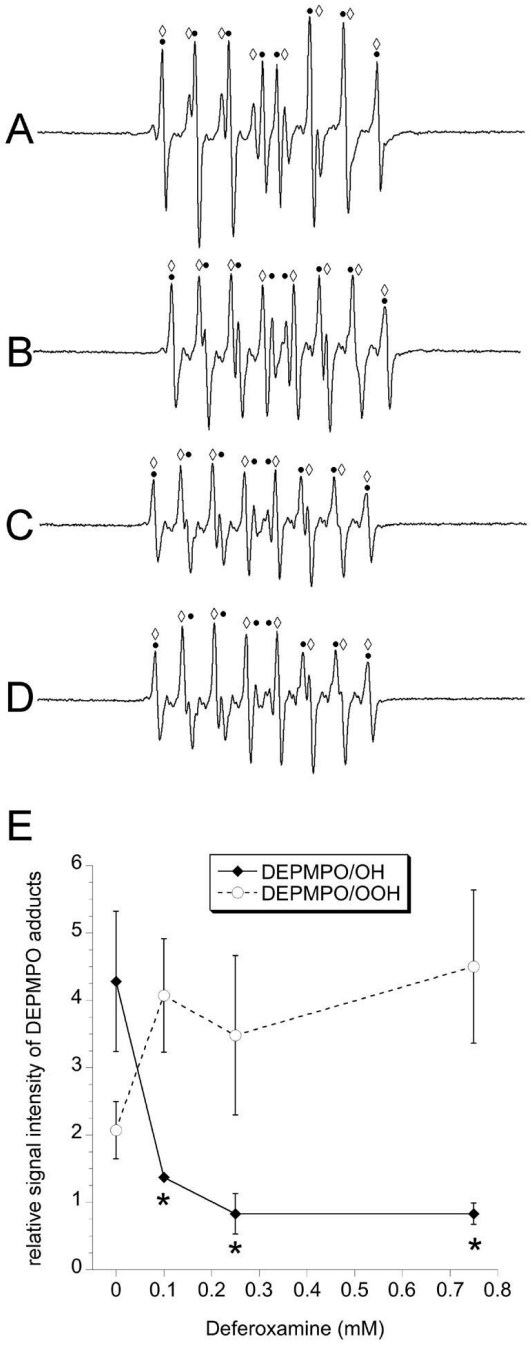


**Fig 6.**

ESR spectra obtained during the NADPH-dependent Cr(VI) reduction catalyzed by proteoliposomes containing cytochrome $b_5$ plus P450 reductase (10 min incubation at 37°C under room air). All samples included DEPMPO (14 mM) plus the following: (A) proteoliposomes plus 50 μM $Na_2CrO_4$ plus the NADPH-generating mix; (B, C, and D) same as A except that deferoxamine (DFX) was included at a concentration of 0.1, 0.25, and 0.75 mM, respectively. Each spectrum represents the average of triplicate experiments. For each, the total reaction volume was 0.25 ml and the amount of proteoliposomes added contained 0.0475 nmol cytochrome $b_5$. Instrument settings were the same as for Fig. 4 except that the microwave power was 19.92 mW; number of scans, 9.

(E) The relative amounts of the spin adducts (mean ± S.D.) determined from the spectra of triplicate experiments with varied levels of DFX. *, significantly different from the samples without DFX ($P < 0.001$).

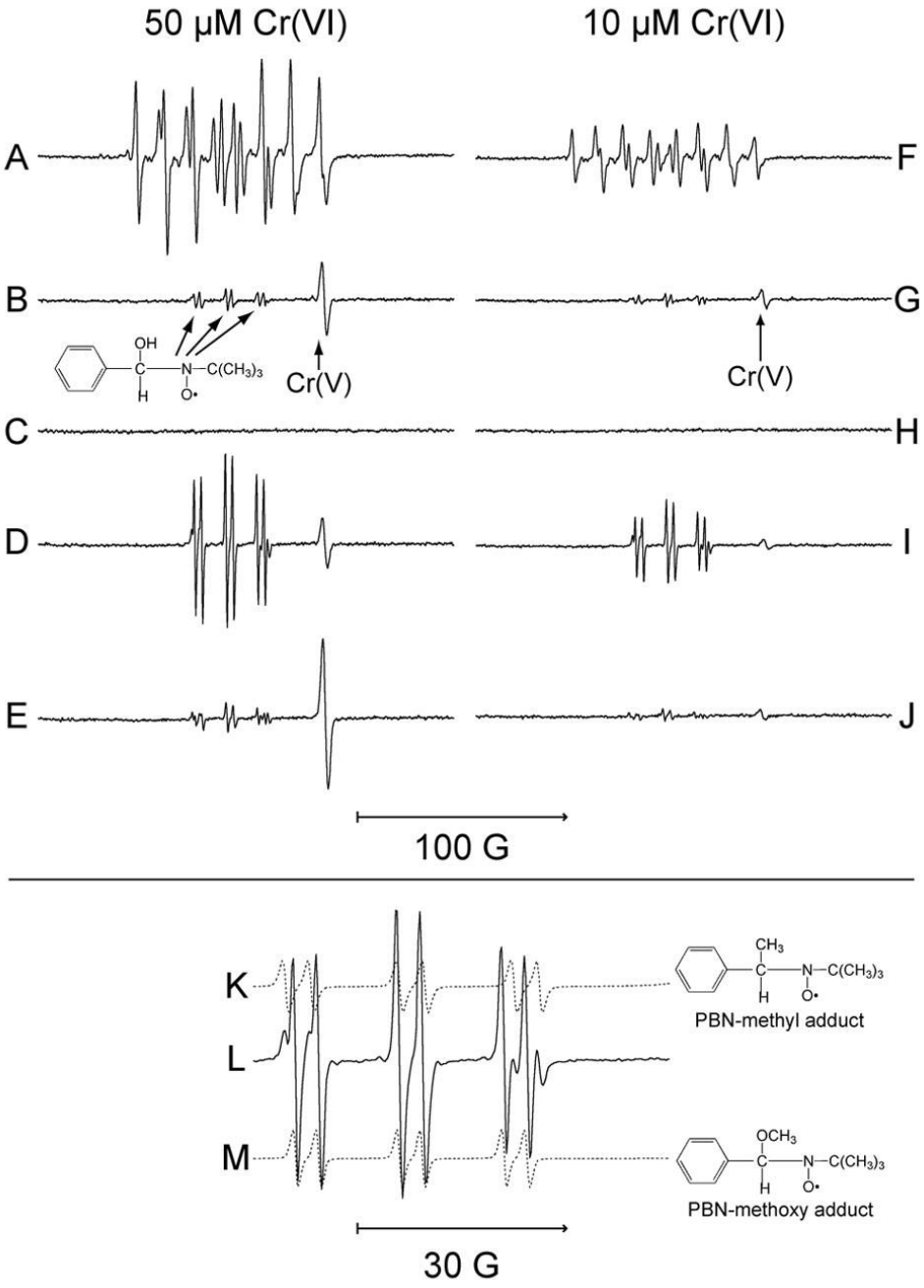


**Fig 7.**

Representative ESR spectra obtained during the NADPH-dependent Cr(VI) reduction catalyzed by proteoliposomes containing cytochrome $b_5$ plus P450 reductase (10 min incubation at 37°C under room air). Samples included: (A) proteoliposomes, 50 μM Cr(VI), the NADPH-generating mix, and 14 mM DEPMPO; (B) same as A except 50 mM PBN was substituted for DEPMPO; (C) same as B but without the NADPH-generating mix; (D) same as B plus 0.70 M DMSO; (E) same as D plus catalase (550 U, Sigma C100); (F through J) same as A through E, respectively, except that the initial Cr(VI) was 10 μM.

(K) Computer simulation of the PBN/$^{\bullet}CH_3$ adduct spectrum using the hyperfine splitting constants $a^N$ = 16.51 G, $a^H$ = 3.68 G; (L) The same as D except that 100 μM Cr(VI) was used

and the x-axis was expanded to see the central region of the spectrum in finer detail; (M) computer simulation of the PBN/$^{\bullet}OCH_3$ adduct spectrum using the hyperfine splitting constants $a^N$ = 15.05 G, $a^H$ = 3.32 G.

For each, the total reaction volume was 0.25 ml and the amount of proteoliposomes added contained 0.0475 nmol cytochrome $b_5$. The instrument settings were the same as for Fig. 4; number of scans, 9.

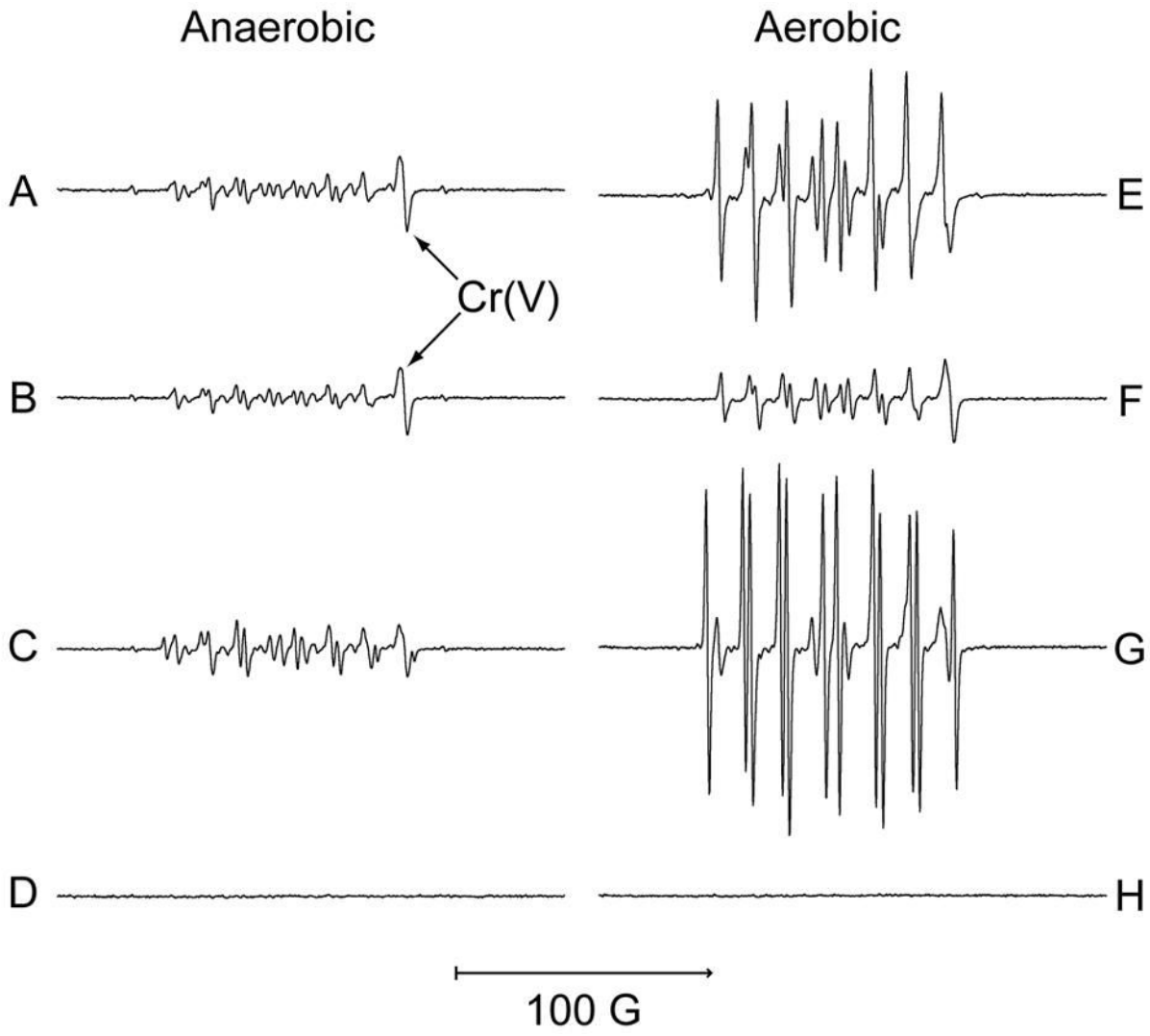


**Fig 8.**

ESR spectra obtained during the NADPH-dependent Cr(VI) reduction catalyzed by proteoliposomes containing cytochrome $b_5$ plus P450 reductase (10 min incubation at 37°C). Reactions were incubated in the anaerobic chamber (A to D) or under room air (E to H). All samples included DEPMPO (14 mM), 100 μM $Na_2CrO_4$, proteoliposomes, and the following: (A) the NADPH-generating mix; (B) same as A plus catalase (550 U, Sigma C100); (C) same as A plus ammonium formate (250 mM); (D) same as A but without the NADPH-generating mix; (E, F, G, and H) same as A, B, C, and D, respectively, except that incubation was under room air. For each, the total reaction volume was 0.25 ml and the amount of proteoliposomes added contained 0.0475 nmol cytochrome $b_5$. Instrument settings were as follows: 1 G modulation amplitude, 19.92 mW microwave power, $6.32 \times 10^4$ receiver gain, 40.96 msec time constant, 9.76 GHz microwave frequency, sweep width = 200 G, field set = 3480 G, modulation frequency = 100 kHz, scan time = 42 sec; number of scans, 9.

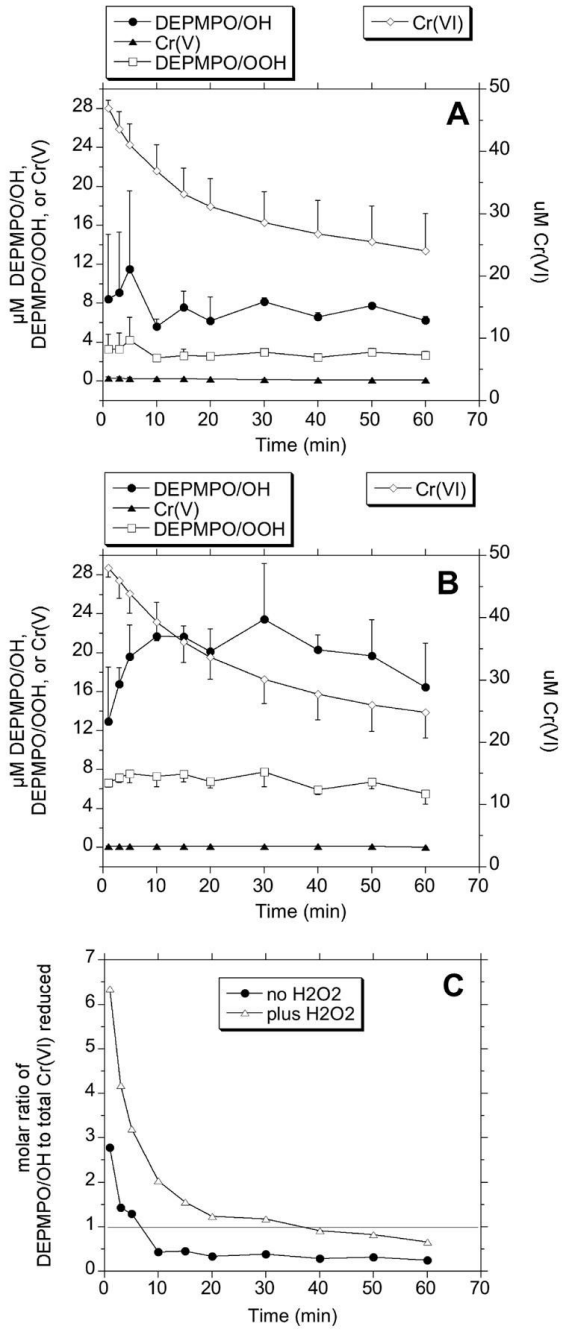


**Fig 9.**

Time course analysis of ESR spectra and net change in Cr(VI) levels during the NADPH-dependent Cr(VI) reduction catalyzed by proteoliposomes containing cytochrome $b_5$ plus P450 reductase (incubation at 37°C under room air). The samples included proteoliposomes, 50 µM Cr(VI), the NADPH-generating mix, and 14 mM DEPMPO. The experiments were conducted either (A) without added $H_2O_2$, or (B) with the addition of 2 mM $H_2O_2$. Note that the scale for Cr(VI) (right) is different than that for the other species (left). Points represent the means of three independent experiments, and the error bars represent the standard deviation. The error bars are shown in one direction only to avoid visual confusion for some of the time points. For each, the total reaction volume was 0.25 ml and the amount of proteoliposomes

added contained 0.0475 nmol cytochrome $b_5$. The ESR instrument settings were the same as for Fig. 4; number of scans, 9. (C) The data from panels A and B were used to calculate the molar ratio of DEPMPO/$^{\bullet}$OH adduct at each time point relative to the net total decline in Cr (VI) concentration from time zero.